Electronic Supporting information

Multi-Step Solvent-Free Mechanochemical Route to Indium(III) Complexes

Jingyi Wang,[a] Rakesh Ganguly,[a] Li Yongxin,[a] Jesus Díaz,[b,] Han Sen Soo*[†a,c,d] and Felipe García*[†a]

[a.] Division of Chemistry and Biological Chemistry, School of Physical and Mathematical Sciences, Nanyang Technological University, 21 Nanyang Link 637371, Singapore.
[b.] Departamento de Química Orgánica e Inorgánica, Facultad de Veterinaria, Universidad de Extremadura, Cáceres 10071, Spain
[c.] Singapore-Berkeley Research Initiative for Sustainable Energy (SinBeRISE), 1 Create Way, Singapore 138602.
[d.] Solar Fuels Laboratory, Nanyang Technological University, 50 Nanyang Avenue, Singapore 639798.
† These authors jointly supervised this work.

Experimental section

General considerations

All reactions were carried out in a stainless steel grinder jar using a Mixer Mill MM400 machine. The recrystallization of products was performed under a dry and inert atmosphere by using a combination of standard Schlenk line techniques and a Vacuum Atmospheres N_2 glovebox. Solvents including tetrahydrofuran (THF), diethyl ether (Et_2O) and pentane were distilled over Na/benzophenone and degassed using freeze-pump-thaw cycles prior to use. Anhydrous acetonitrile (ACN) were collected from a PURE SOLV MD-5 solvent purification system and stored in a glovebox. Anhydrous 1,2-dimethoxyethane (DME) and dichloromethane (DCM) were distilled over calcium hydride (CaH_2) and stored in a glovebox. Anhydrous *N*,*N*-dimethylformamide (DMF) in a Sure-Seal bottle was purchased from Sigma-Aldrich and used as received. Deuterated chloroform ($CDCl_3$) and acetonitrile (CD_3CN) were distilled over CaH_2 and stored over 4 Å molecular sieves. Deuterated acetone was distilled over K_2CO_3. All reagents were purchased from commercial sources and were used without further purification.

The ^1H and $^{13}C\{^1H\}$ NMR spectra were recorded at 298 K on a Bruker Avance DPX400 and DPX300 spectrometer. The chemical shift values are reported in parts per million (ppm) relative to TMS, using residual protonated solvents as the internal standards (^1H: δ = 7.26 for $CDCl_3$ and δ = 1.94 for CD_3CN; ^{13}C: δ = 77.2 for $CDCl_3$ and δ = 118.3 for CD_3CN). The ^{115}In spectra were recorded on a JEOL ECA400 spectrometer, using a 0.5 M D_2O solution of

$In(NO_3)_3$ as the external standard. No internal standards were used for the ^{115}In NMR spectra. UV-Vis absorption measurements were carried out on a Shimadzu UV-3600 spectrophotometer. Crystallographic data were recorded on a Bruker X8 CCD diffractometer. High-resolution ESI mass spectra were obtained using a Waters Q-Tof Premier.

Mechanochemical synthesis of BIAN ligands

(a) Synthesis of *p*-MeOAr-BIAN (1)

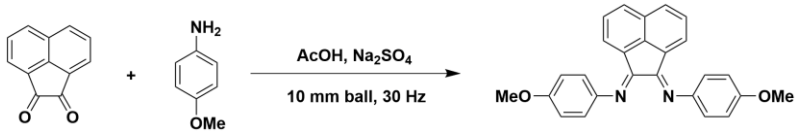

Scheme S1. Mechanochemical synthesis of the *p*-MeOAr-BIAN **(1)**.

A stainless steel grinder jar was dried in an oven at 120 ºC overnight prior to use. The grinder jar was charged with acenaphthoquinone (0.073 g, 0.40 mmol), *p*-anisidine (0.099 g, 0.80 mmol), acetic acid (5.7 µL, 0.10 mmol, 25 mol%), and Na_2SO_4 (0.014 g, 0.10 mmol, 25 mol%), and equipped with a 10 mm stainless steel ball. The jar was then grinded for 3.5 h at 30 Hz. The resultant red powder was dissolved in dichloromethane (DCM), filtered, and the filtrate was concentrated and washed with pentane. The crude product was recrystallized by layering a THF solution of the product beneath pentane and the isolated yield was 0.13 g (84%). ^1H NMR (400 MHz, $CDCl_3$): δ = 3.90 (s, 6 H), 7.01 - 7.04 (m, 6 H), 7.09 - 7.11 (m, 4 H), 7.39 (t, J = 8.0 Hz, 2 H), 7.89 (d, J = 8.4 Hz, 2 H). $^{13}C\{^1H\}$ NMR (100 MHz, $CDCl_3$): δ = 55.7, 114.8, 119.9, 123.8, 127.7, 128.9, 129.0, 131.4, 141.8, 145.1, 157.1, 161.7. HRMS (ESI+, m/z) calculated for $C_{26}H_{21}N_2O_2$ $[M + H]^+$ m/z = 393.1603, found 393.1595.

(b) Synthesis of *p*-BrAr-BIAN (2)

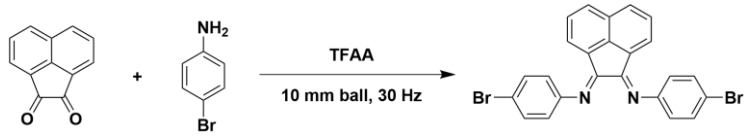

Scheme S2. Mechanochemical synthesis of the *p*-BrAr-BIAN **(2)**.

A stainless steel grinder jar was dried in an oven at 120 ºC overnight prior to use. The grinder jar was charged with acenaphthoquinone (0.073 g, 0.40 mmol), *p*-bromoaniline (0.17 g, 1.0 mmol) and trifluoroacetic anhydride (14.1 µL, 0.10 mmol, 25 mol%), and equipped with a 10 mm stainless steel ball. The jar was then grinded for 3 h at 30 Hz. The resultant yellow solid

was washed with Et_2O. The crude product was recrystallized by layering a DCM solution of the product beneath pentane and the isolated yield was 0.13 g (64%). ^{1}H NMR (300 MHz, $CDCl_3$): δ = 6.96 - 7.05 (m, 6 H), 7.45 (t, J = 7.5 Hz, 2 H), 7.60 (d, J = 8.7 Hz, 4 H), 7.94 (d, J = 8.1 Hz, 2 H). ^{13}C{^{1}H} NMR (100 MHz, $CDCl_3$): δ = 117.7, 120.3, 124.2, 127.9, 128.3, 129.6, 131.4, 132.7, 142.1, 150.6, 161.6. HRMS (ESI+, m/z) calculated for $C_{24}H_{15}N_2{}^{79}Br^{81}Br$ $[M + H]^+$ m/z = 490.9581, found 490.9574.

Mechanochemical synthesis of indium complexes

(a) [(*p*-MeOAr-BIAN)$_2$InCl$_2$][InCl$_4$] (3)

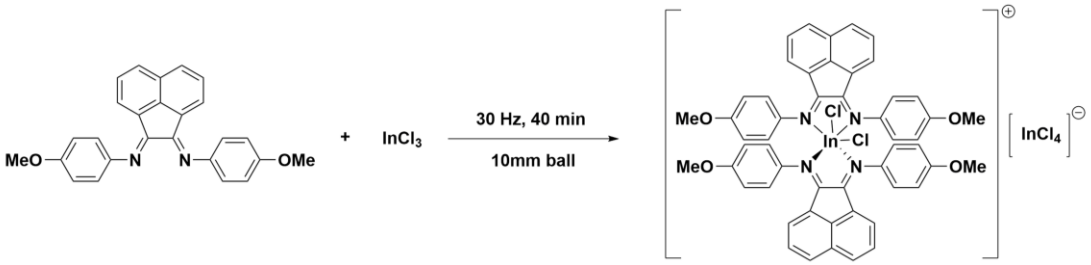

Scheme S3. Mechanochemical synthesis of [(*p*-MeOAr-BIAN)$InCl_2$][$InCl_4$] **(3)**.

A stainless steel grinder jar was dried in an oven at 120 ºC overnight prior to use. The grinder jar was charged with *p*-MeOAr-BIAN (0.039 g, 0.10 mmol) and $InCl_3$ (0.022 g, 0.10 mmol), and equipped with a 10 mm stainless steel ball. The jar was then grinded in air for 40 min at 30 Hz. The resultant red solid was purified by washing with Et_2O and the isolated yield was 0.044 g (72%). The purity of the product was confirmed by elemental analysis. (Anal. Calcd. for $C_{26}H_{20}N_2O_2InCl_3$: C, 50.89; H, 3.29; N, 4.57. Found: C, 50.78; H, 3.45; N, 4.44.) Recrystallization by vapor diffusion of Et_2O into an ACN solution of the red solid resulted in single crystals suitable for single crystal X-ray analysis. ^{1}H NMR (400 MHz, acetone-d_6, -75 °C, *trans*-isomer): δ = 3.90 (s, 12 H), 6.0 (d, J = 8.2 Hz, 4 H), 7.05 (d, J = 8.8 Hz, 4 H), 7.25-7.29 (m, 16 H), 8.45 (d, J = 8.4 Hz, 4 H). ^{13}C{^{1}H} NMR (100 MHz, acetone-d_6, 25 °C): δ = 56.2, 56.4, 115.7, 116.4 (broad, may have peaks overlapping), 124.5 (broad, may have peaks overlapping), 124.7, 126.1, 127.2, 127.4, 128.2, 130.0, 130.3, 132.3, 133.4, 134.6, 137.1, 138.5, 146.0, 160.7, 161.4, 162.7. ^{115}In NMR (86 MHz, acetonitrile-d_3, 25 °C): δ = 452.7. HRMS (ESI+, m/z) calculated for $C_{52}H_{40}N_4O_4InCl_2$ $[M]^+$ m/z = 969.1465, found 969.1418. Anal. Calcd. for $C_{26}H_{20}N_2O_2InCl_3$: C, 50.89; H, 3.29; N, 4.57. Found: C, 50.59; H, 3.09; N, 4.57.

(b) (*p*-BrAr-BIAN)$InCl_3$•DMF (4)

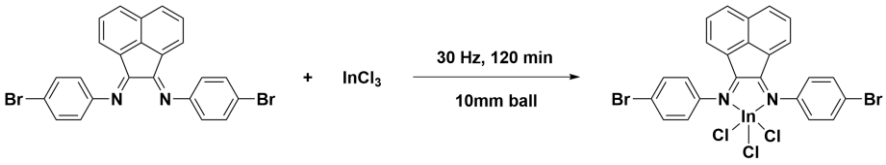

Scheme S4: Mechanochemical synthesis of (*p*-BrAr-BIAN)$InCl_3$ **(4)**.

A stainless steel grinder jar was dried in an oven at 120 ºC overnight prior to use. The grinder jar was charged with *p*-BrAr-BIAN (0.049 g, 0.10 mmol) and $InCl_3$ (0.022 g, 0.10 mmol), and equipped with a 10 mm stainless steel ball. The jar was then grinded under Ar atmosphere for 120 min at 30 Hz. The resultant yellow solid was purified by washing with DCM and the isolated yield was 84%. The purity of the product was confirmed by elemental analysis. (Anal. Calcd. for $C_{24}H_{14}Br_2Cl_3InN_2 \cdot H_2O$: C, 39.52; H, 2.21; N, 3.84. Found: C, 39.40; H, 2.17; N, 3.69.) Recrystallization by vapour diffusion of Et_2O into a DMF solution of the yellow solid resulted in single crystals suitable for single crystal X-ray analysis. ^{1}H NMR (400 MHz, acetone-d_6, -25 °C): δ = 7.16 (s, broad, 2 H), 7.43 (m. 4 H), 7.78 (t, J = 8.0 Hz, 2 H), 7.83 (d, J = 7.6 Hz, 4 H), 8.40 (d, J = 8.4 Hz, 2 H). The ^{13}C{^{1}H} NMR could not be obtained due to the poor solubility of **4** in most of the deuterated solvents. HRMS (ESI+, *m/z*) calculated for $C_{24}H_{15}N_2{}^{81}Br_2{}^{113}InCl_3$ $[M+H]^+$ *m/z* = 710.7667, found 710.7686. Anal. Calcd. for $C_{24}H_{14}Br_2Cl_3InN_2 \cdot 2$ DMF: C, 42.02; H, 3.29; N, 6.53. Found: C, 42.04; H, 3.15; N, 6.19.

One-pot mechanochemical synthesis of indium complexes

(a) Complex 3

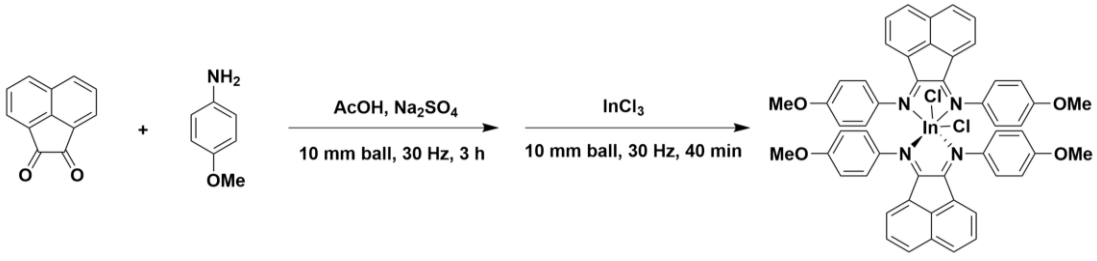

Scheme S5: One-pot mechanochemical synthesis of complex **3**.

A stainless steel grinder jar was dried in an oven at 120 ºC overnight prior to use. The grinder jar was charged with acenaphthoquinone (0.036 g, 0.20 mmol), *p*-anisidine (0.049 g, 0.20 mmol), acetic acid (2.9 µL, 0.050 mmol, 25 mol%), and Na_2SO_4 (0.0071 g, 0.05

mmol, 25 mol%), and equipped with a 10 mm stainless steel ball. The jar was then grinded for 3 h at 30 Hz. To the resultant red powder, $InCl_3$ (0.044 g, 0.20 mmol) was added in the glovebox and the mixture was further grinded for 40 min. The resultant red solid was recrystallized by vapour diffusion of Et_2O into an ACN solution of the crude product and the isolated yield was 0.048 g (57%). A unit cell measurement was performed on a single crystal grown from this reaction and it was found to be indistinguishable from those obtained by isolating **1** first.

(b) Complex 4

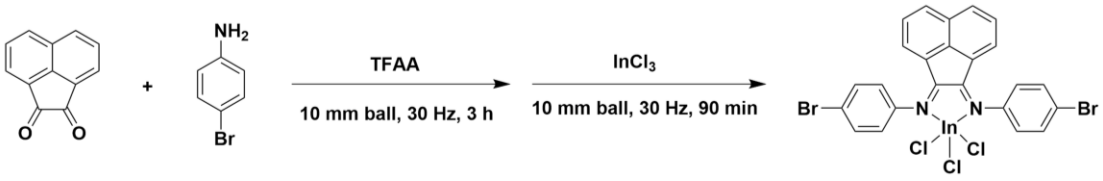

Scheme S6: One-pot mechanochemical synthesis of complex **4**.

A stainless steel grinder jar was dried in an oven at 120 ºC overnight prior to use. The grinder jar was charged with acenaphthoquinone (0.036 g, 0.20 mmol), *p*-bromoaniline (0.069 g, 0.20 mmol), and trifluoroacetic anhydride (7.1 µL, 0.050 mmol, 25 mol%), and equipped with a 10 mm stainless steel ball. The jar was then grinded for 3 h at 30 Hz. To the resultant khaki powder, $InCl_3$ (0.044 g, 0.20 mmol) was added in the glovebox and the mixture was further grinded for 90 min. The resultant orange solid was recrystallized by vapor diffusion of Et_2O into a DMF solution of the crude product. The product formed was confirmed by single crystal X-ray data. A unit cell measurement was performed on a single crystal grown from this reaction and it was found to be indistinguishable from those obtained by isolating **2** first.

Synthesis of Ar-BIAN ligands in solution phase

The method for the synthesis of **1** and **2** in solution were adapted from previous lieterature.[1,2] references 1 and 2 respectively. The isolated yield obtained were 95% for **1** and 46% for **2** respectively.

Synthesis of indium(III) complexes in solution phase

(a) Complex 3

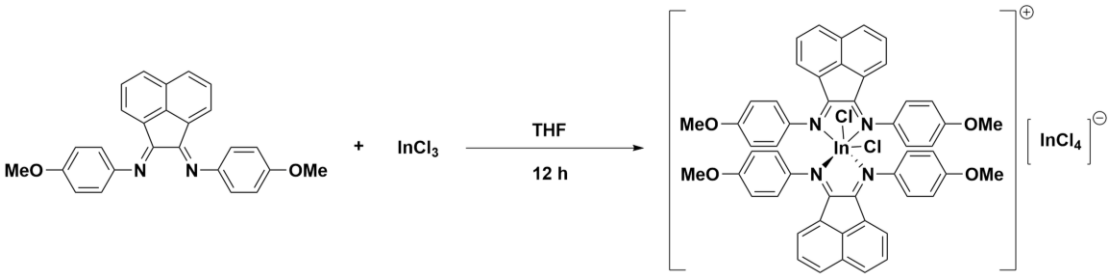

Scheme S7: Synthesis of complex **3** in solution phase.

A solution of $InCl_3$ (0.044 g, 0.20 mmol) in THF (10 ml) was added to a solution of *p*-MeOAr-BIAN (0.076 g, 0.20 mmol) in THF (3 ml) at room temperature. The resulting red suspension was stirred overnight, after which all volatiles were removed under vacuum. The product was recrystallized by vapor diffusion of Et_2O into an ACN solution of the crude red solid and the isolated yield was 0.10 g (81%). This afforded red crystalline blocks suitable for single crystal X-ray analysis. All other analysis data are identical to those obtained from the mechanochemical approach.

(b) Complex 4

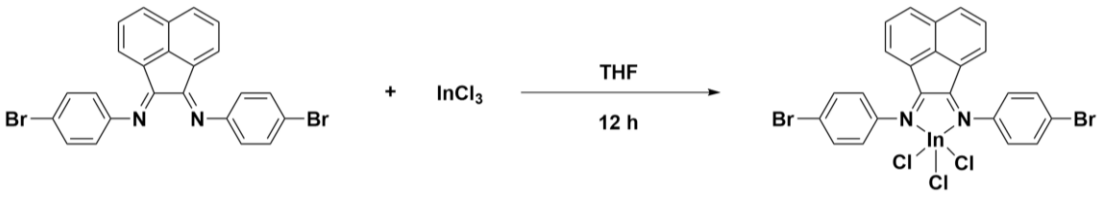

Scheme S8: Synthesis of complex **4** in solution phase.

A solution of $InCl_3$ (0.022g, 0.10 mmol) in THF (5 ml) was added to a solution of *p*-BrAr-BIAN (0.049g, 0.10 mmol) in THF (5 ml) at room temperature. The resulting yellow suspension was stirred overnight, after which all volatiles were removed under vacuum. The product was recrystallized by vapour diffusion of Et_2O into a DMF solution of the crude yellow solid and the isolated yield was 0.044 g (61%). This afforded yellow crystals suitable for single crystal X-ray analysis. All other analysis data are identical to that obtained from the mechanochemical approach.

Single crystal X-ray structure of compounds

Complex 3

A red block-like specimen of $C_{26}H_{20}Cl_3InN_2O_2$, with approximate dimensions of 0.320 mm x 0.360 mm x 0.420 mm, was used for the X-ray crystallographic analysis. The X-ray intensity data were measured. The total exposure time was 0.34 hours. The frames were integrated with the Bruker SAINT Software package using a narrow-frame algorithm. The integration of the data using a triclinic unit cell yielded a total of 72379 reflections to a maximum θ angle of 31.11° (0.69 Å resolution), of which 15605 were independent (average redundancy = 4.638, completeness = 99.4%, R_{int} = 5.47%, R_{sig} = 4.82%), and 12545(80.39%) were greater than $2\sigma(F^2)$. The final cell constants of a = 9.6102(4) Å, b = 15.9145(7) Å, c = 17.2004(8) Å, α = 79.7863(13)°, β = 76.3618(14)°, γ = 74.1154(12)°, volume = 2440.90(19) $Å^3$, are based upon the refinement of the XYZ-centroids of 9940 reflections above 20 σ(I) with 4.495° < 2θ < 59.80°. Data were corrected for absorption effects using the multi-scan method (SADABS). The ratio of minimum to maximum apparent transmission was 0.829. The calculated minimum and maximum transmission coefficients (based on crystal size) are 0.6060 and 0.6770. The final anisotropic full-matrix least-squares refinement on F^2 with 617 variables converged at R1 = 3.21% for the observed data, and wR2 = 6.63% for all data. The goodness-of-fit was 1.024. The largest peak in the final difference electron density synthesis was 0.728 $e^-/Å^3$ and the largest hole was -0.557 $e^-/Å^3$ with an RMS deviation of 0.108 $e^-/Å^3$. On the basis of the final model, the calculated density was1.670 g/cm^3 and F(000), 1224 e^-.

Complex 4

An orange plate-like specimen of $C_{30}H_{28}Br_2Cl_3InN_4O_2$, with approximate dimensions of 0.060 mm x 0.140 mm x 0.200 mm, was used for the X-ray crystallographic analysis. The X-ray intensity data were measured. The total exposure time was 1.06 hours. The frames were integrated with the Bruker SAINT software package using a narrow-frame algorithm. The integration of the data using a monoclinic unit cell yielded a total of 77866 reflections to a maximum θ angle of 31.11° (0.69 Å resolution), of which 10081 were independent (average redundancy = 7.724, completeness = 99.2%, R_{int} = 9.80%, R_{sig} = 6.44%), and 7395(73.36%) were greater than $2\sigma(F^2)$. The final cell constants of a = 12.4120(10) Å, b = 19.7758(15) Å, c = 13.5227(10) Å, β = 107.797(3)°, volume = 3160.4(4) $Å^3$, are based upon the refinement of the XYZ-centroids

of 9224 reflections above 20 σ(I) with 4.411° < 2θ < 56.84°. Data were corrected for absorption effects using the multi-scan method (SADABS). The ratio of minimum to maximum apparent transmission was 0.792. The calculated minimum and maximum transmission coefficients (based on crystal size) are 0.5360 and 0.8150. The final anisotropic full-matrix least-squares refinement on F^2 with 383 variables converged at R1 = 3.88% for the observed data, and wR2 = 11.51% for all data. The goodness-of-fit was 1.058. The largest peak in the final difference electron density synthesis was 1.246 $e^-/Å^3$ and the largest hole was -0.961 $e^-/Å^3$ with an RMS deviation of 0.181 $e^-/Å^3$. On the basis of the final model, the calculated density was 1.802 g/cm^3 and F(000), 1688 e^-.

X-ray crystallographic coordinates for structures

Complexes **3** and **4** reported herein have been deposited with the Cambridge Crystallographic Data Centre (CCDC), under deposition numbers CCDC 1439070-1439071. These data can be obtained free of charge from the Cambridge Crystallographic Data Centre via www.ccdc.cam.ac.uk/data_request/cif.

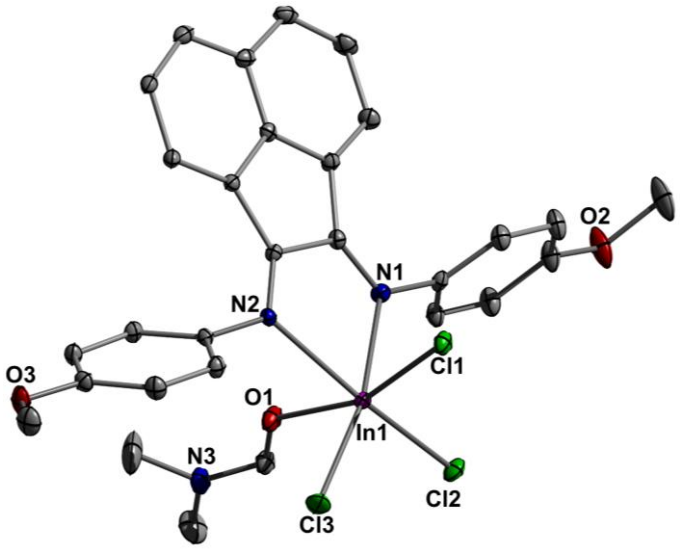

Fig. S1 The crystal structure of **3b** obtained by recrystallization from vapour diffusion of Et_2O into a DMF solution of the product. When the product was dissolved in ACN, structure shown in **3a** was obtained since the six coordination sites need to be occupied around the indium(III) centre. When the product was dissolved in DMF, the strongly coordinating DMF molecule facilitates the formation of six-coordinated indium complex, resulting in structure shown in **3b**.

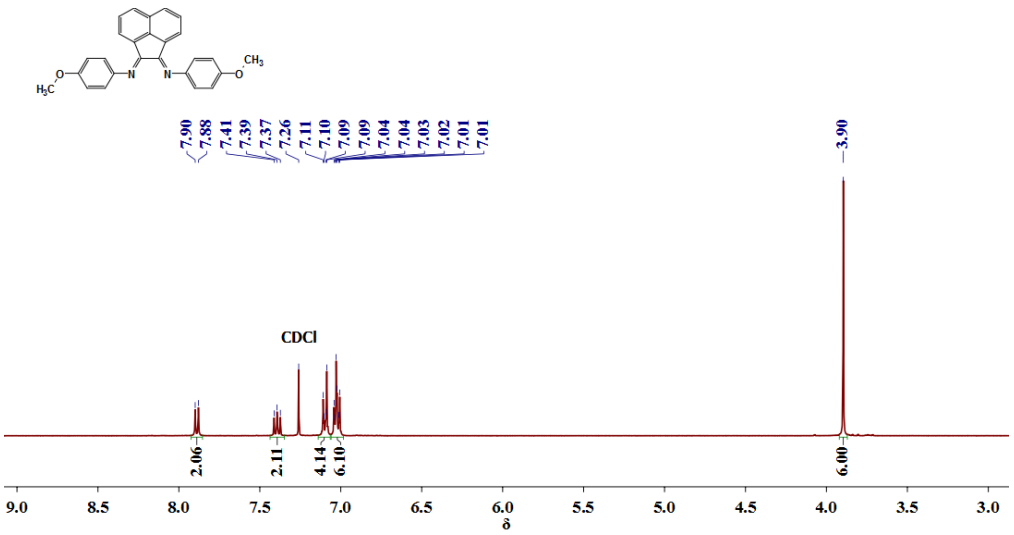

Fig. S2 The ^{1}H NMR spectrum of **1** recorded in $CDCl_3$.

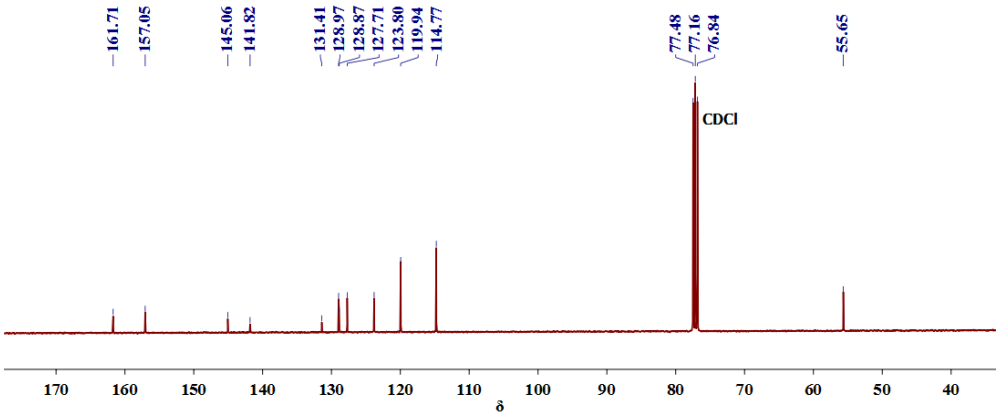

Fig. S3 The ^{13}C NMR spectrum of **1** recorded in $CDCl_3$.

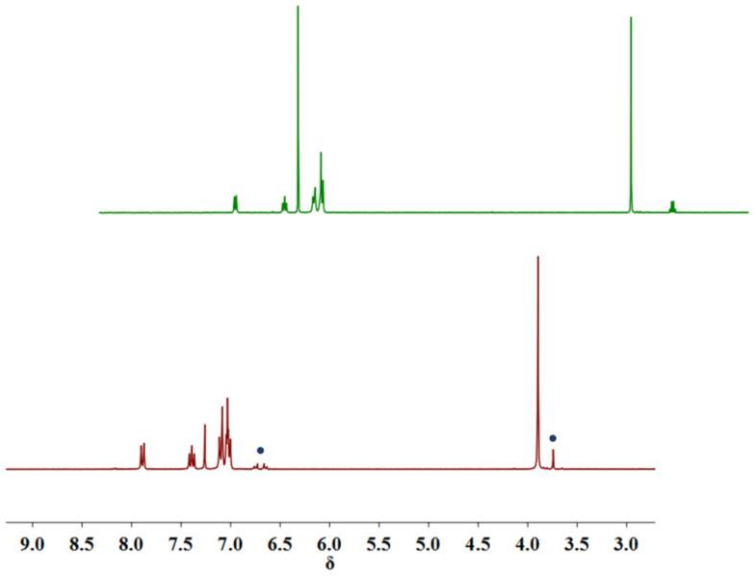

Fig. S4 The ^{1}H NMR spectrum of **1** recorded in $CDCl_3$ before purification (top: $ZnCl_2$-templated synthesis in acetic acid; bottom: mechanochemical synthesis). Blue circles indicate unreacted *p*-anisidine.

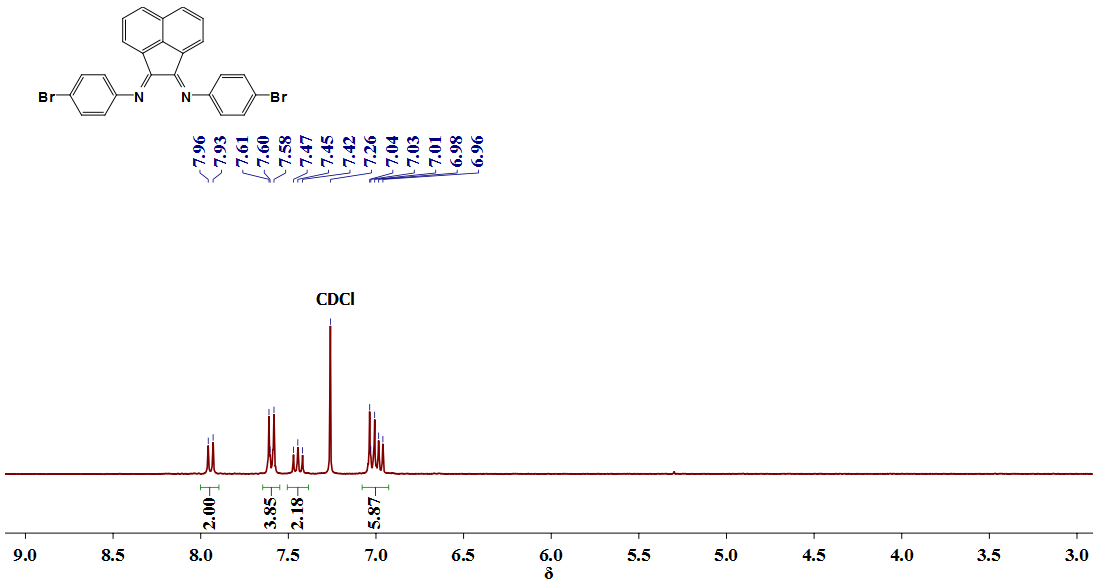

Fig. S5 The ^{1}H NMR spectrum of **2** recorded in $CDCl_3$.

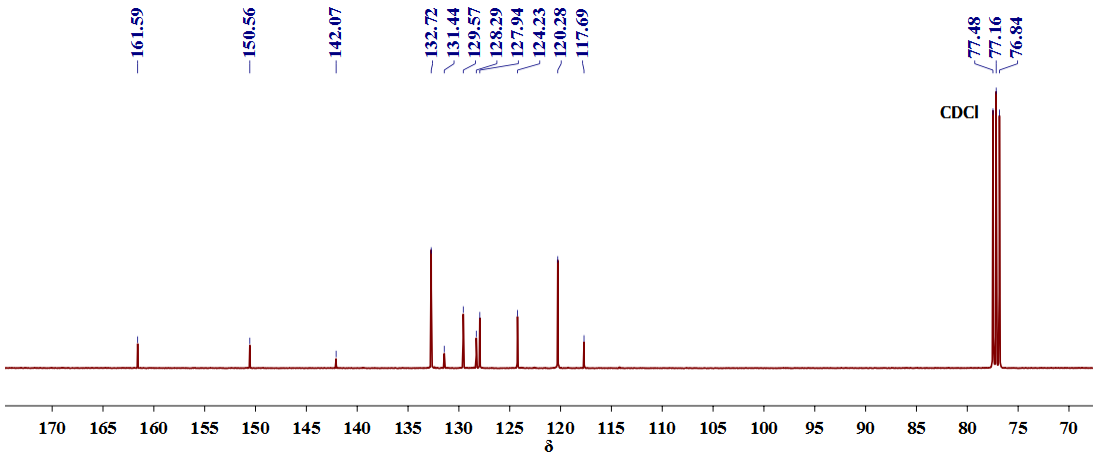

Fig. S6 The ^{13}C NMR spectrum of **2** recorded in $CDCl_3$.

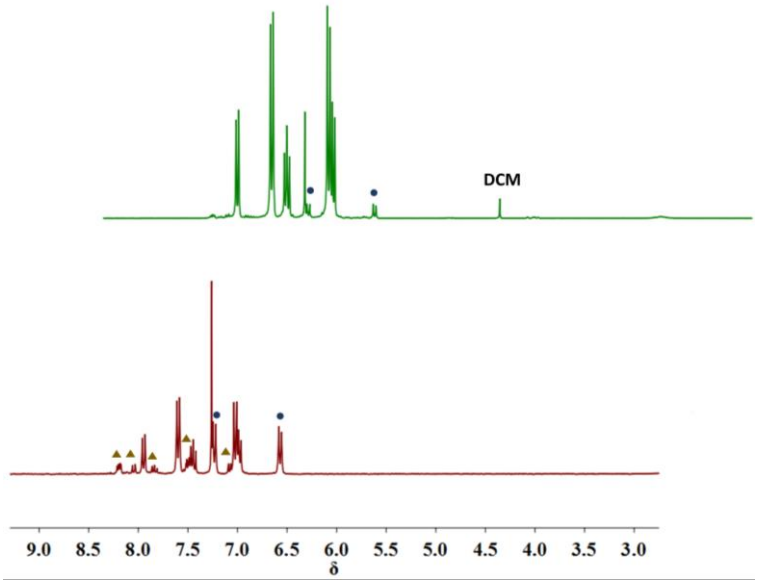

Fig. S7 The ^{1}H NMR spectrum of **2** recorded in $CDCl_3$ before purification (top: $ZnCl_2$-templated synthesis in acetic acid; bottom: mechanochemical synthesis). Blue circles indicate unreacted *p*-bromoaniline and gold triangles indicate mono-imine side products.

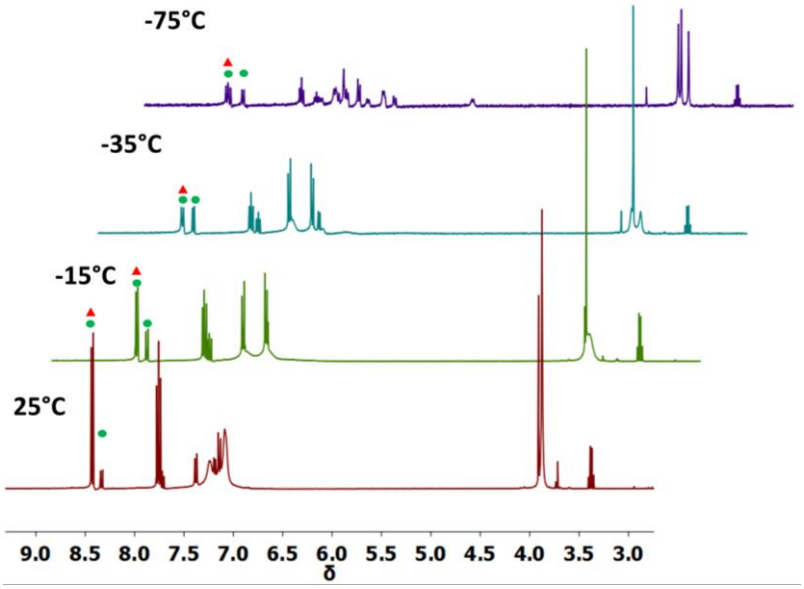

Fig. S8 ^{1}H NMR in acetone-d_6 of **3** at 25 ˚C, -15 ˚C, -35 ˚C and -75 ˚C. (marked peaks were used for Van't Hoff plot, green circle: *cis*-isomer; red triangle: *trans*-isomer). At -15 ˚C, the *trans*- and *cis*-isomers are present in a 1.8:1 ratio. As the temperature reached -35˚C, this ratio changed to 0.87:1 and appeared to level off as 0.99:1 at -75 ˚C.

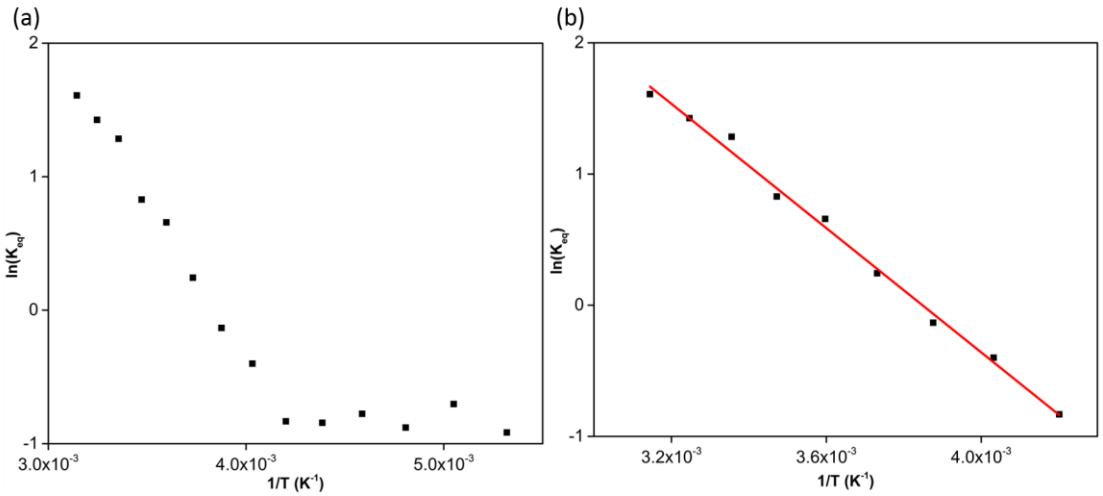

Fig. S9 Van't Hoff plots for **3a** recorded in acetone-d_6 (a) from -85 °C to 45 °C and (b) linear fit from -35 °C to 45 °C (ln K_{eq} = –2370/T + 9.11).

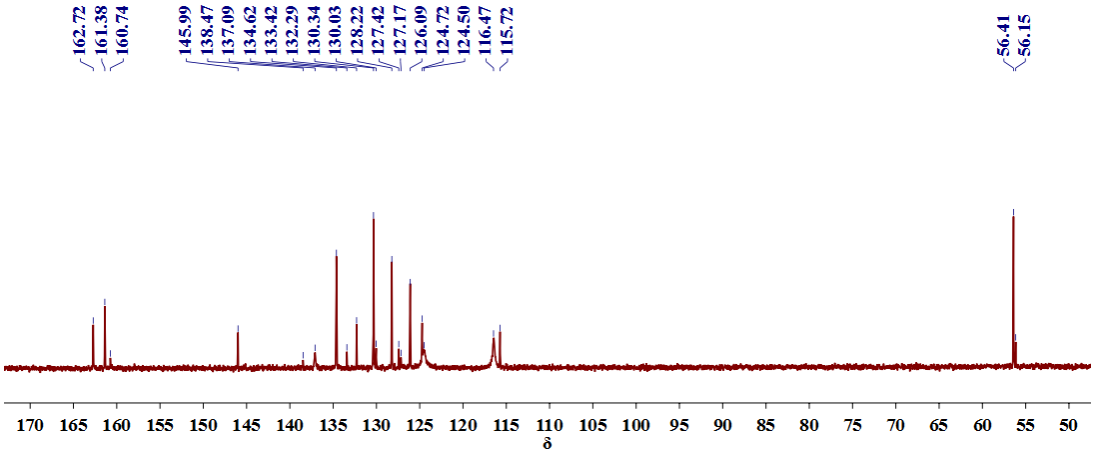

Fig. S10 The ^{13}C NMR spectrum of **3a** recorded in acetone-d_6 at 25 °C.

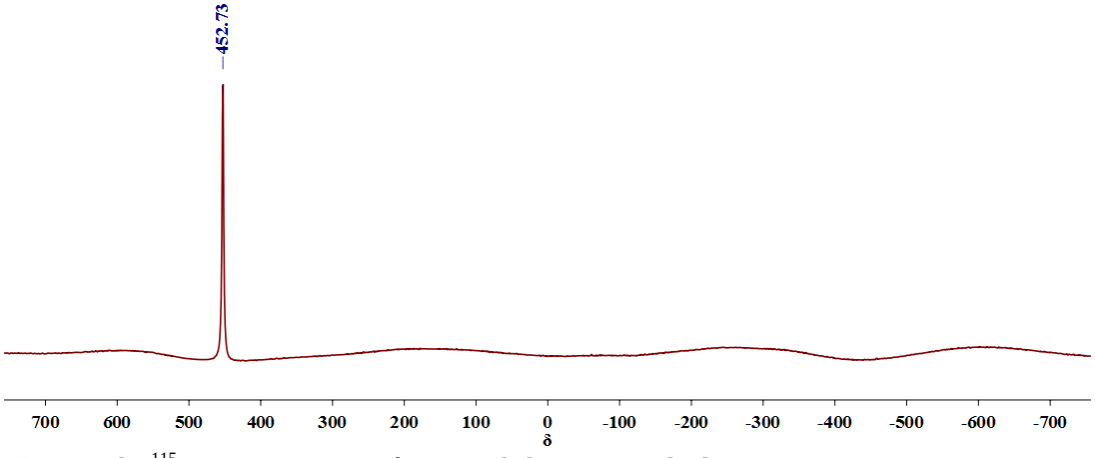

Fig. S11 The ^{115}In NMR spectrum of **3a** recorded in acetonitrile-d_3 at 25 °C.

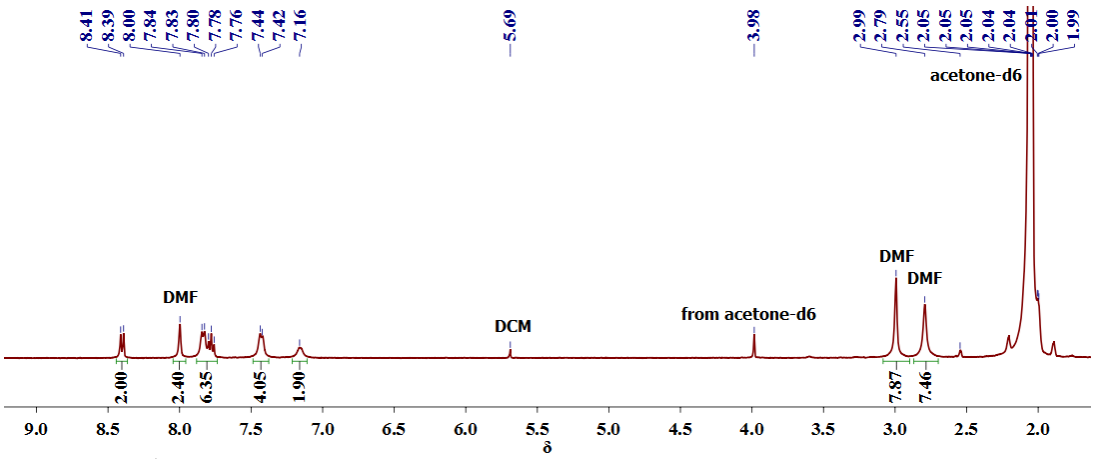

Fig. S12 The ^{1}H NMR spectrum of **4** recorded in acetone-d_6 at -25 °C

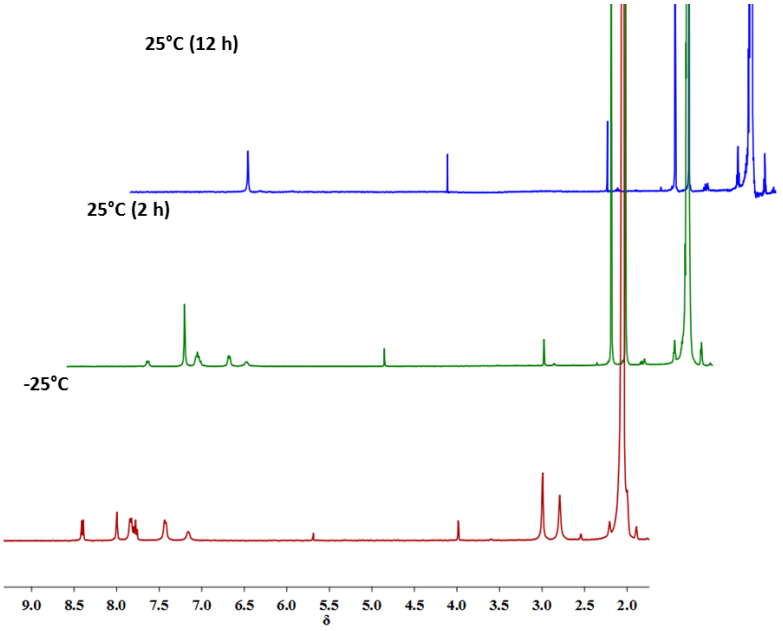

Fig. S13 The ^{1}H NMR spectrum of **4** recorded in acetone-d_6 at -25 °C (red), after standing at 25 °C for 2 h (green), and after standing at 25 °C overnight (blue), showing the decomposition of **4** at room temperature.

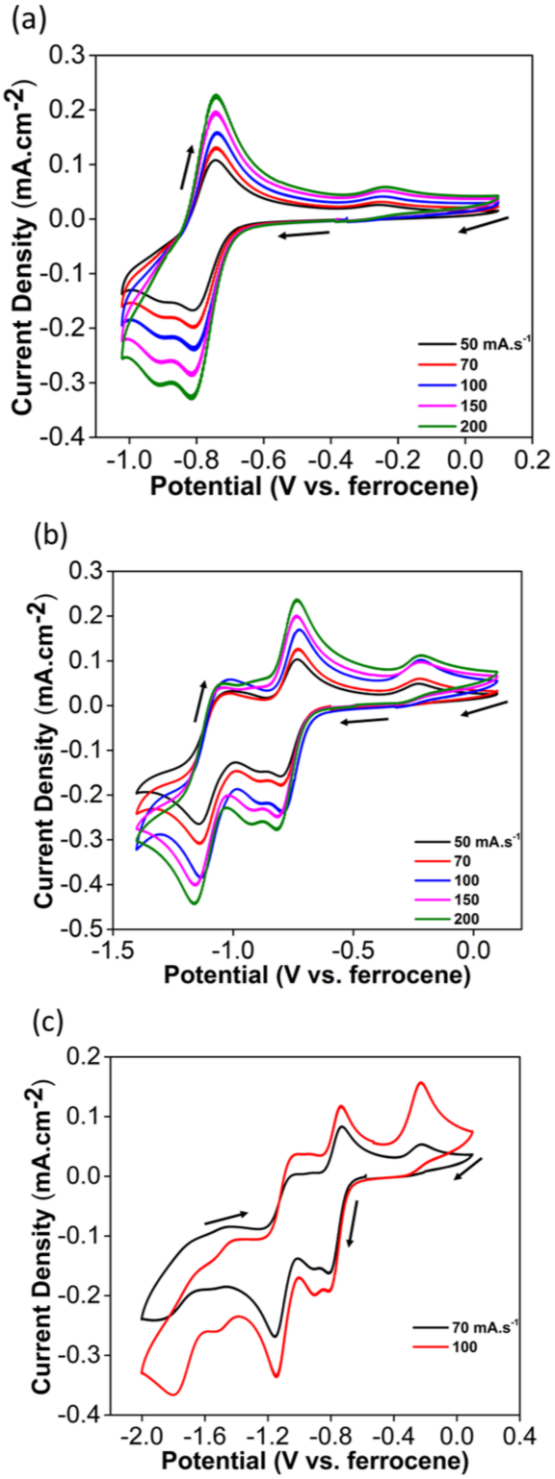

Fig. S14 The (a) first and second, (b) third and (c) fourth and fifth reduction waves in the CVs for 2.1 mM of **3a** in 0.10 M (nBu$_4$N)PF$_6$ in ACN with a glassy carbon electrode (3 mm in diameter) at different scan rates. The peak-to-peak separation and the ratio of anodic to cathodic current change when the scan rate is decreased to 70 mA.s^{-1} for the fourth of fifth reduction, highlighting the chemically irreversible nature of these two reductions.

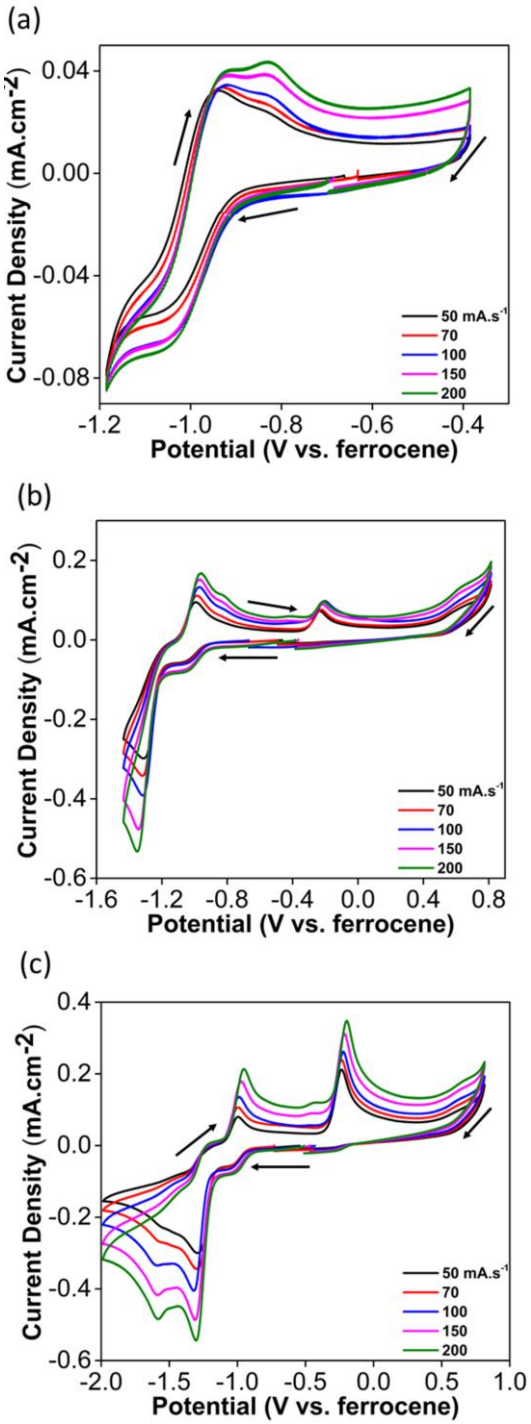

Fig. S15 The (a) first, (b) second and (c) third reduction waves in the CVs for 2.2 mM of **4** in 0.10 M (nBu$_4$N)PF$_6$ in DMF with a glassy carbon electrode (3 mm in diameter) at different scan rates.

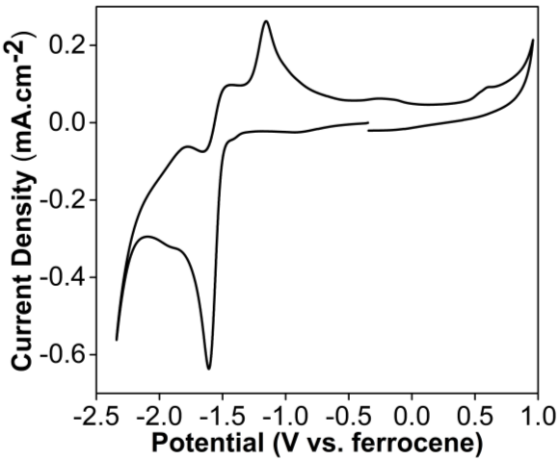

Fig. S16 CV for 2.0 mM of **2** in 0.10 M (nBu$_4$N)PF$_6$ in DMF with a glassy carbon electrode (3 mm in diameter) at a scan rate of 100 mV s^{-1}.

X-Ray data of compounds

Table S1 X-ray crystallographic and refinement data for complex **3a**

Chemical formula	$C_{26}H_{20}Cl_3InN_2O_2$
Formula weight	613.61 g/mol
Temperature	103(2) K
Wavelength	0.71073 Å
Crystal size	0.320 x 0.360 x 0.420 mm
Crystal habit	red block
Crystal system	triclinic
Space group	P -1
Unit cell dimensions	a = 9.6102(4) Å α = 79.7863(13)˚
	b = 15.9145(7) Å β = 76.3618(14)˚
	c = 17.2004(8) Å γ = 74.1154(12)˚
Volume	2440.90(19) $Å^3$
Z	4
Density (calculated)	1.670 g/cm^3
Absorption coefficient	1.324 mm^{-1}
F(000)	1224
Theta range for data collection	2.94 to 31.11°
Index ranges	-13<=h<=13, -23<=k<=23, -24<=l<=24
Reflections collected	72379
Independent reflections	15605 [R(int) = 0.0547]
Coverage of independent reflections	99.4%
Absorption correction	multi-scan
Max. and min. transmission	0.6770 and 0.6060
Refinement method	Full-matrix least-squares on F^2
Refinement program	SHELXL-2014/6 (Sheldrick, 2014)
Function minimized	$\Sigma\, w(F_o^2 - F_c^2)^2$
Data / restraints / parameters	15605 / 0 / 617
Goodness-of-fit on F^2	1.024
Δ/σ_{max}	0.002
	12545
Final R indices	data; R1 = 0.0321, wR2 = 0.0605
	I>2σ(I)
	all data R1 = 0.0469, wR2 = 0.0663
Weighting scheme	$w=1/[\sigma^2(F_o^2)+(0.0191P)^2+1.4807P]$
	where $P=(F_o^2+2F_c^2)/3$
Largest diff. peak and hole	0.728 and -0.557 $eÅ^{-3}$
R.M.S. deviation from mean	0.108 $eÅ^{-3}$

Table S2 Selected bond lengths (Å) for complex **3**

In1-N1	2.2955(16)	In1-N3	2.3109(17)
In1-N4	2.3232(16)	In1-N2	2.3241(16)
Cl1-In1	2.4126(5)	Cl2-In1	2.3963(5)
C8-N1	1.282(2)	C8-C19	1.520(3)
C19-N2	1.280(2)	C34-N3	1.279(3)
C34-C45	1.523(3)	C45-N4	1.291(3)

Table S3 Selected bond angles (°C) for complex **3**

N1-In1-N3	85.77(6)	N1-In1-N4	153.02(6)
N3-In1-N4	72.68(6)	N1-In1-N2	73.35(6)
N3-In1-N2	78.37(6)	N4-In1-N2	86.29(6)
N1-In1-Cl2	97.51(4)	N3-In1-Cl2	168.79(4)
N4-In1-Cl2	100.86(4)	N2-In1-Cl2	92.25(4)
N1-In1-Cl1	100.73(4)	N3-In1-Cl1	89.51(4)
N4-In1-Cl1	95.24(4)	N2-In1-Cl1	166.76(4)
Cl2-In1-Cl1	100.345(19)		

Table S4 Atomic coordinates and equivalent isotropic atomic displacement parameters ($Å^2$) for complex **3**

	x/a	y/b	z/c	U(eq)
C1	0.0691(3)	0.64074(19)	0.31967(15)	0.0302(6)
C2	0.8479(2)	0.68261(13)	0.41657(12)	0.0135(4)
C3	0.9157(2)	0.72265(13)	0.45775(12)	0.0135(4)
C4	0.8353(2)	0.75983(13)	0.52725(12)	0.0123(4)
C5	0.6866(2)	0.76122(13)	0.55240(11)	0.0105(4)
C6	0.6190(2)	0.72040(13)	0.51174(12)	0.0108(4)
C7	0.6998(2)	0.68054(13)	0.44472(12)	0.0132(4)
C8	0.4835(2)	0.85938(12)	0.62411(12)	0.0095(4)
C9	0.3995(2)	0.90736(13)	0.56175(12)	0.0116(4)
C10	0.4232(2)	0.91260(13)	0.47892(12)	0.0144(4)
C11	0.3151(2)	0.97015(14)	0.43829(13)	0.0165(4)
C12	0.1864(2)	0.02036(14)	0.47896(13)	0.0170(4)
C13	0.1599(2)	0.01788(13)	0.56390(13)	0.0145(4)
C14	0.0359(2)	0.06800(14)	0.61312(14)	0.0167(4)
C15	0.0285(2)	0.06222(14)	0.69484(14)	0.0172(4)
C16	0.1411(2)	0.00689(13)	0.73342(13)	0.0150(4)
C17	0.2606(2)	0.95555(13)	0.68733(12)	0.0115(4)
C18	0.2691(2)	0.96151(13)	0.60307(12)	0.0121(4)
C19	0.3973(2)	0.89256(13)	0.70341(12)	0.0105(4)
C20	0.3729(2)	0.89187(13)	0.84373(12)	0.0110(4)
C21	0.2474(2)	0.86224(14)	0.88370(12)	0.0145(4)
C22	0.1733(2)	0.88858(14)	0.95791(13)	0.0148(4)
C23	0.2216(2)	0.94565(13)	0.99263(12)	0.0121(4)
C24	0.1860(3)	0.02480(14)	0.10417(13)	0.0182(5)
C25	0.3476(2)	0.97382(13)	0.95339(12)	0.0131(4)
C26	0.4243(2)	0.94600(13)	0.87903(12)	0.0123(4)
C27	0.1712(2)	0.54820(16)	0.54732(14)	0.0213(5)
C28	0.3574(2)	0.56822(13)	0.60728(12)	0.0126(4)
C29	0.5004(2)	0.53483(13)	0.62235(12)	0.0137(4)
C30	0.5476(2)	0.57204(13)	0.67476(12)	0.0129(4)
C31	0.4519(2)	0.64201(13)	0.71383(12)	0.0112(4)
C32	0.3124(2)	0.67740(14)	0.69640(13)	0.0150(4)
C33	0.2643(2)	0.64070(14)	0.64301(13)	0.0146(4)
C34	0.4520(2)	0.65298(13)	0.84818(12)	0.0098(4)
C35	0.3488(2)	0.59925(13)	0.89081(12)	0.0113(4)
C36	0.2689(2)	0.55172(13)	0.86628(13)	0.0140(4)
C37	0.1885(2)	0.50062(14)	0.92638(14)	0.0164(4)
C38	0.1861(2)	0.49753(13)	0.00716(13)	0.0153(4)
C39	0.2692(2)	0.54381(13)	0.03348(13)	0.0128(4)
C40	0.2848(2)	0.54108(13)	0.11409(13)	0.0148(4)
C41	0.3799(2)	0.58378(14)	0.13013(13)	0.0151(4)
C42	0.4631(2)	0.63269(13)	0.06889(12)	0.0119(4)
C43	0.4472(2)	0.63902(12)	0.99027(12)	0.0095(4)
C44	0.3498(2)	0.59426(13)	0.97378(12)	0.0101(4)
C45	0.5169(2)	0.67783(12)	0.91106(11)	0.0091(4)
C46	0.7064(2)	0.73553(12)	0.93619(11)	0.0091(4)
C47	0.8600(2)	0.71036(13)	0.91257(12)	0.0109(4)
C48	0.9478(2)	0.71852(13)	0.96240(12)	0.0123(4)
C49	0.8843(2)	0.75421(13)	0.03488(12)	0.0123(4)
C50	0.9252(3)	0.79697(18)	0.15267(14)	0.0260(5)
C51	0.7312(2)	0.78553(13)	0.05541(12)	0.0120(4)
C52	0.6427(2)	0.77584(13)	0.00581(12)	0.0103(4)
Cl1	0.86711(5)	0.62724(3)	0.71842(3)	0.01548(10)
Cl2	0.81612(6)	0.86180(4)	0.73749(3)	0.01804(11)
Cl3	0.35610(6)	0.36732(3)	0.75861(3)	0.01926(11)
Cl4	0.68452(6)	0.19415(4)	0.81786(3)	0.02286(12)
Cl5	0.68225(6)	0.26577(4)	0.59285(3)	0.02062(11)

Cl6	0.41805(7)	0.12582(4)	0.72323(3)	0.02343(12)
In1	0.67286(2)	0.75729(2)	0.74681(2)	0.00917(3)
In2	0.53330(2)	0.23949(2)	0.72053(2)	0.01375(4)
N1	0.60604(18)	0.80124(11)	0.62352(10)	0.0099(3)
N2	0.45227(18)	0.86434(11)	0.76679(10)	0.0110(3)
N3	0.50116(18)	0.67354(11)	0.77335(10)	0.0113(3)
N4	0.62284(18)	0.71731(11)	0.88526(10)	0.0095(3)
O1	0.91635(17)	0.64296(11)	0.34903(9)	0.0213(4)
O2	0.13643(16)	0.97000(10)	0.06432(8)	0.0149(3)
O3	0.32087(16)	0.52437(10)	0.55690(9)	0.0166(3)
O4	0.98196(16)	0.75659(10)	0.07948(9)	0.0173(3)

Table S5 Anisotropic atomic displacement parameters ($Å^2$) for complex **3**
The anisotropic atomic displacement factor exponent takes the form: $-2\pi^2[h^2 a^{*2} U_{11} + ... + 2 h k a^* b^* U_{12}]$

	U_{11}	U_{22}	U_{33}	U_{23}	U_{13}	U_{12}
C1	0.0183(12)	0.0491(17)	0.0204(12)	-0.0181(12)	0.0069(10)	-0.0039(11)
C2	0.0160(10)	0.0137(10)	0.0081(9)	-0.0020(7)	-0.0007(8)	-0.0001(8)
C3	0.0096(9)	0.0153(10)	0.0126(10)	-0.0009(8)	0.0005(7)	-0.0012(8)
C4	0.0123(10)	0.0147(10)	0.0110(9)	-0.0024(8)	-0.0032(7)	-0.0040(8)
C5	0.0113(9)	0.0101(9)	0.0077(9)	-0.0004(7)	-0.0003(7)	-0.0004(7)
C6	0.0108(9)	0.0102(9)	0.0112(9)	0.0011(7)	-0.0032(7)	-0.0025(7)
C7	0.0160(10)	0.0128(9)	0.0120(9)	-0.0028(8)	-0.0045(8)	-0.0031(8)
C8	0.0099(9)	0.0087(9)	0.0098(9)	-0.0027(7)	0.0004(7)	-0.0031(7)
C9	0.0128(10)	0.0095(9)	0.0130(9)	-0.0014(7)	-0.0030(8)	-0.0031(7)
C10	0.0171(11)	0.0127(9)	0.0130(10)	-0.0027(8)	-0.0033(8)	-0.0020(8)
C11	0.0245(12)	0.0143(10)	0.0122(10)	-0.0002(8)	-0.0079(9)	-0.0044(9)
C12	0.0201(11)	0.0135(10)	0.0194(11)	-0.0009(8)	-0.0109(9)	-0.0020(8)
C13	0.0151(10)	0.0114(9)	0.0174(10)	-0.0016(8)	-0.0048(8)	-0.0025(8)
C14	0.0135(10)	0.0125(10)	0.0237(11)	-0.0018(8)	-0.0051(9)	-0.0016(8)
C15	0.0128(10)	0.0140(10)	0.0225(11)	-0.0047(9)	-0.0011(8)	0.0004(8)
C16	0.0144(10)	0.0138(10)	0.0160(10)	-0.0035(8)	-0.0008(8)	-0.0030(8)
C17	0.0108(9)	0.0108(9)	0.0127(9)	-0.0013(7)	-0.0015(7)	-0.0031(7)
C18	0.0116(10)	0.0107(9)	0.0147(10)	-0.0016(8)	-0.0032(8)	-0.0033(7)
C19	0.0102(9)	0.0106(9)	0.0104(9)	-0.0028(7)	0.0005(7)	-0.0031(7)
C20	0.0107(9)	0.0114(9)	0.0093(9)	-0.0018(7)	-0.0009(7)	-0.0004(7)
C21	0.0161(10)	0.0154(10)	0.0140(10)	-0.0044(8)	-0.0011(8)	-0.0071(8)
C22	0.0138(10)	0.0173(10)	0.0139(10)	-0.0023(8)	0.0007(8)	-0.0073(8)
C23	0.0125(10)	0.0119(9)	0.0097(9)	-0.0021(7)	-0.0014(7)	0.0006(8)
C24	0.0253(12)	0.0186(11)	0.0124(10)	-0.0068(8)	0.0014(9)	-0.0094(9)
C25	0.0150(10)	0.0136(9)	0.0122(9)	-0.0038(8)	-0.0025(8)	-0.0049(8)
C26	0.0108(10)	0.0130(9)	0.0128(10)	-0.0024(8)	-0.0001(7)	-0.0041(8)
C27	0.0199(12)	0.0255(12)	0.0238(12)	-0.0073(10)	-0.0106(9)	-0.0059(9)
C28	0.0157(10)	0.0138(9)	0.0100(9)	-0.0019(7)	-0.0024(8)	-0.0064(8)
C29	0.0161(10)	0.0125(9)	0.0127(10)	-0.0042(8)	-0.0017(8)	-0.0031(8)
C30	0.0130(10)	0.0152(10)	0.0107(9)	-0.0014(8)	-0.0016(8)	-0.0045(8)
C31	0.0129(10)	0.0141(9)	0.0087(9)	-0.0009(7)	-0.0008(7)	-0.0079(8)
C32	0.0126(10)	0.0160(10)	0.0169(10)	-0.0049(8)	-0.0030(8)	-0.0024(8)
C33	0.0126(10)	0.0157(10)	0.0166(10)	-0.0035(8)	-0.0041(8)	-0.0032(8)
C34	0.0088(9)	0.0100(9)	0.0117(9)	-0.0034(7)	-0.0037(7)	-0.0012(7)
C35	0.0081(9)	0.0116(9)	0.0137(9)	-0.0030(7)	0.0003(7)	-0.0028(7)
C36	0.0099(10)	0.0143(10)	0.0177(10)	-0.0045(8)	-0.0020(8)	-0.0020(8)
C37	0.0089(10)	0.0143(10)	0.0268(12)	-0.0058(9)	-0.0026(8)	-0.0029(8)
C38	0.0098(10)	0.0123(10)	0.0224(11)	-0.0002(8)	0.0003(8)	-0.0044(8)
C39	0.0086(9)	0.0116(9)	0.0155(10)	-0.0008(8)	0.0003(7)	-0.0007(7)
C40	0.0141(10)	0.0126(9)	0.0136(10)	0.0010(8)	0.0027(8)	-0.0027(8)
C41	0.0165(11)	0.0153(10)	0.0110(10)	-0.0005(8)	-0.0007(8)	-0.0019(8)
C42	0.0108(9)	0.0121(9)	0.0118(9)	-0.0017(7)	-0.0005(7)	-0.0026(7)
C43	0.0081(9)	0.0089(9)	0.0100(9)	-0.0016(7)	0.0002(7)	-0.0011(7)

C44	0.0069(9)	0.0097(9)	0.0121(9)	-0.0013(7)	0.0009(7)	-0.0018(7)
C45	0.0087(9)	0.0088(9)	0.0086(9)	-0.0015(7)	-0.0008(7)	-0.0010(7)
C46	0.0105(9)	0.0105(9)	0.0081(9)	0.0006(7)	-0.0026(7)	-0.0057(7)
C47	0.0129(10)	0.0093(9)	0.0107(9)	-0.0017(7)	-0.0011(7)	-0.0039(7)
C48	0.0088(9)	0.0134(9)	0.0151(10)	0.0004(8)	-0.0026(8)	-0.0043(7)
C49	0.0142(10)	0.0133(9)	0.0127(9)	0.0014(8)	-0.0059(8)	-0.0078(8)
C50	0.0254(13)	0.0428(15)	0.0162(11)	-0.0091(11)	-0.0063(10)	-0.0138(11)
C51	0.0155(10)	0.0114(9)	0.0103(9)	-0.0020(7)	-0.0023(8)	-0.0053(8)
C52	0.0103(9)	0.0099(9)	0.0102(9)	-0.0009(7)	-0.0005(7)	-0.0032(7)
Cl1	0.0120(2)	0.0155(2)	0.0163(2)	-0.00328(19)	0.00019(18)	-0.00080(18)
Cl2	0.0220(3)	0.0198(3)	0.0171(2)	0.0006(2)	-0.0056(2)	-0.0131(2)
Cl3	0.0211(3)	0.0155(2)	0.0204(3)	-0.0053(2)	-0.0059(2)	0.0004(2)
Cl4	0.0207(3)	0.0263(3)	0.0173(3)	-0.0055(2)	-0.0063(2)	0.0052(2)
Cl5	0.0166(3)	0.0300(3)	0.0154(2)	-0.0009(2)	0.0000(2)	-0.0098(2)
Cl6	0.0304(3)	0.0198(3)	0.0209(3)	-0.0062(2)	0.0054(2)	-0.0141(2)
In1	0.00884(7)	0.01180(7)	0.00734(6)	-0.00158(5)	-0.00101(5)	-0.00352(5)
In2	0.01467(8)	0.01388(7)	0.01209(7)	-0.00248(5)	-0.00074(6)	-0.00350(6)
N1	0.0108(8)	0.0101(8)	0.0092(8)	-0.0012(6)	-0.0005(6)	-0.0043(6)
N2	0.0109(8)	0.0134(8)	0.0084(8)	-0.0036(6)	0.0003(6)	-0.0030(6)
N3	0.0112(8)	0.0126(8)	0.0117(8)	-0.0038(6)	-0.0019(6)	-0.0044(7)
N4	0.0096(8)	0.0097(8)	0.0089(8)	-0.0015(6)	-0.0021(6)	-0.0013(6)
O1	0.0178(8)	0.0301(9)	0.0149(8)	-0.0132(7)	0.0036(6)	-0.0033(7)
O2	0.0161(8)	0.0181(7)	0.0105(7)	-0.0062(6)	0.0015(6)	-0.0047(6)
O3	0.0168(8)	0.0200(8)	0.0171(8)	-0.0085(6)	-0.0063(6)	-0.0049(6)
O4	0.0142(8)	0.0281(9)	0.0135(7)	-0.0043(6)	-0.0051(6)	-0.0082(6)

Table S6 X-ray crystallographic and refinement data for complex **4**

Chemical formula	$C_{30}H_{28}Br_2Cl_3InN_4O_2$
Formula weight	857.55 g/mol
Temperature	103(2) K
Wavelength	0.71073 Å
Crystal size	0.060 x 0.140 x 0.200 mm
Crystal habit	orange plate
Crystal system	monoclinic
Space group	P 1 21/c 1
Unit cell dimensions	a = 12.4120(10) Å α = 90˚ b = 19.7758(15) Å β = 107.797(3)˚ c = 13.5227(10) Å γ = 90˚
Volume	3160.4(4) $Å^3$
Z	4
Density (calculated)	1.802 g/cm^3
Absorption coefficient	3.565 mm^{-1}
F(000)	1688
Theta range for data collection	1.72 to 31.11°
Index ranges	-18<=h<=18, -28<=k<=28, -19<=l<=17
Reflections collected	77866
Independent reflections	10081 [R(int) = 0.0980]
Coverage of independent reflections	99.2%
Absorption correction	multi-scan
Max. and min. transmission	0.8150 and 0.5360
Refinement method	Full-matrix least-squares on F^2
Refinement program	SHELXL-2014/6 (Sheldrick, 2014)
Function minimized	$\Sigma w(F_o^2 - F_c^2)^2$
Data / restraints / parameters	10081 / 0 / 383
Goodness-of-fit on F^2	1.058
Δ/σ_{max}	0.001
	7395
Final R indices	data; R1 = 0.0388, wR2 = 0.0905

	I>2σ(I) all data R1 = 0.0686, wR2 = 0.1151
Weighting scheme	$w=1/[\sigma^2(F_o^2)+(0.0576P)^2]$ where $P=(F_o^2+2F_c^2)/3$
Largest diff. peak and hole	1.246 and -0.961 eÅ^{-3}
R.M.S. deviation from mean	0.181 eÅ^{-3}

Table S7 Selected bond lengths (Å) for complex **4**

In1-O1	2.258(2)	In1-N2	2.301(3)
In1-N1	2.390(3)	In1-Cl2	2.4185(9)
In1-Cl3	2.4286(9)	In1-Cl1	2.4336(9)
C17-N2	1.279(4)	C7-N1	1.282(4)
C7-C17	1.521(4)		

Table S8 Selected bond angles (°C) for complex **4**

O1-In1-N2	78.20(9)	O1-In1-N1	79.31(9)
N2-In1-N1	72.22(9)	O1-In1-Cl2	94.67(6)
N2-In1-Cl2	162.92(7)	N1-In1-Cl2	91.31(7)
O1-In1-Cl3	86.69(6)	N2-In1-Cl3	96.34(7)
N1-In1-Cl3	163.40(7)	Cl2-In1-Cl3	98.74(3)
O1-In1-Cl1	163.65(6)	N2-In1-Cl1	86.51(7)
N1-In1-Cl1	90.60(7)	Cl2-In1-Cl1	98.43(3)
Cl3-In1-Cl1	100.88(3)	C7-N1-In1	113.1(2)
C17-N2-In1	116.1(2)		

Table S9 Atomic coordinates and equivalent isotropic atomic displacement parameters (Å^2) for complex **4**

	x/a	**y/b**	**z/c**	**U(eq)**
In1	0.30344(2)	0.46191(2)	0.25841(2)	0.01103(6)
Br1	0.31636(3)	0.79171(2)	0.58595(3)	0.02439(10)
Br2	0.95324(3)	0.20748(2)	0.87032(3)	0.01929(9)
C1	0.2264(3)	0.59145(15)	0.3972(3)	0.0116(6)
C2	0.3051(3)	0.58992(16)	0.4945(3)	0.0131(6)
C3	0.3322(3)	0.64951(17)	0.5533(3)	0.0156(7)
C4	0.2811(3)	0.70959(16)	0.5105(3)	0.0153(7)
C5	0.2050(3)	0.71161(16)	0.4113(3)	0.0174(7)
C6	0.1761(3)	0.65221(17)	0.3552(3)	0.0182(7)
C7	0.0919(3)	0.50879(15)	0.3196(3)	0.0115(6)
C8	0.9964(3)	0.52872(15)	0.3557(3)	0.0120(6)
C9	0.9839(3)	0.57178(16)	0.4314(3)	0.0142(7)
C10	0.8762(3)	0.57636(17)	0.4469(3)	0.0171(7)
C11	0.7843(3)	0.54008(17)	0.3868(3)	0.0193(7)
C12	0.7949(3)	0.49453(17)	0.3105(3)	0.0149(7)
C13	0.7084(3)	0.45258(18)	0.2441(3)	0.0190(7)
C14	0.7333(3)	0.41078(18)	0.1732(3)	0.0201(8)
C15	0.8424(3)	0.40542(17)	0.1619(3)	0.0174(7)
C16	0.9281(3)	0.44437(16)	0.2258(3)	0.0132(6)
C17	0.0505(3)	0.45162(15)	0.2420(3)	0.0115(6)
C18	0.9029(3)	0.48943(16)	0.2976(3)	0.0124(6)
C19	0.0824(3)	0.37004(16)	0.1283(3)	0.0125(6)
C20	0.0305(4)	0.38954(18)	0.0266(3)	0.0244(9)
C21	0.9923(4)	0.34079(18)	0.9501(3)	0.0250(9)
C22	0.0057(3)	0.27350(17)	0.9767(3)	0.0160(7)
C23	0.0565(3)	0.25332(17)	0.0786(3)	0.0163(7)
C24	0.0961(3)	0.30204(16)	0.1553(3)	0.0151(7)
C25	0.3895(3)	0.37231(16)	0.4583(3)	0.0129(6)

C26	0.2905(3)	0.27427(19)	0.4957(3)	0.0242(8)
C27	0.4938(3)	0.29210(18)	0.5888(3)	0.0215(8)
C28	0.7813(4)	0.6169(2)	0.1381(4)	0.0337(10)
C29	0.6376(5)	0.6630(3)	0.2052(4)	0.0455(13)
C30	0.5859(4)	0.5802(2)	0.0609(4)	0.0416(12)
Cl1	0.24689(8)	0.53177(4)	0.10287(7)	0.02184(19)
Cl2	0.47447(7)	0.52168(4)	0.35119(7)	0.01695(17)
Cl3	0.38864(8)	0.36640(4)	0.19747(7)	0.02228(19)
N1	0.1934(2)	0.53031(13)	0.3371(2)	0.0119(5)
N2	0.1213(2)	0.42081(13)	0.2063(2)	0.0121(5)
N3	0.3911(2)	0.31601(14)	0.5114(2)	0.0133(6)
N4	0.6725(3)	0.61996(18)	0.1351(3)	0.0323(8)
O1	0.3022(2)	0.39628(11)	0.39468(19)	0.0155(5)
O2	0.8585(3)	0.65026(18)	0.2004(3)	0.0434(8)

Table S10 Anisotropic atomic displacement parameters ($Å^2$) for complex **4**
The anisotropic atomic displacement factor exponent takes the form: $-2\pi^2[h^2 a^{*2} U_{11} + ... + 2 h k a^* b^* U_{12}]$

	U_{11}	U_{22}	U_{33}	U_{23}	U_{13}	U_{12}
In1	0.01031(11)	0.01057(11)	0.01133(12)	-0.00021(8)	0.00202(8)	0.00174(8)
Br1	0.0250(2)	0.01670(17)	0.0295(2)	-0.01147(15)	0.00532(17)	-0.00508(14)
Br2	0.0253(2)	0.01670(17)	0.01415(18)	-0.00578(13)	0.00345(14)	-0.00336(14)
C1	0.0139(16)	0.0096(14)	0.0123(16)	-0.0029(12)	0.0056(13)	-0.0005(12)
C2	0.0100(15)	0.0126(15)	0.0160(17)	0.0015(12)	0.0030(13)	0.0000(12)
C3	0.0136(16)	0.0177(16)	0.0135(17)	0.0005(13)	0.0013(13)	-0.0020(13)
C4	0.0129(16)	0.0125(15)	0.0206(19)	-0.0054(13)	0.0052(14)	-0.0027(12)
C5	0.0181(17)	0.0106(15)	0.0201(19)	-0.0004(13)	0.0005(14)	0.0045(13)
C6	0.0211(18)	0.0162(16)	0.0127(18)	-0.0001(13)	-0.0017(14)	0.0035(14)
C7	0.0144(16)	0.0087(14)	0.0100(16)	0.0006(11)	0.0019(12)	0.0014(12)
C8	0.0121(15)	0.0106(14)	0.0130(16)	0.0026(12)	0.0033(12)	0.0041(12)
C9	0.0167(17)	0.0112(15)	0.0145(17)	0.0009(12)	0.0044(13)	0.0010(12)
C10	0.0191(18)	0.0136(15)	0.0217(19)	0.0021(13)	0.0108(15)	0.0036(13)
C11	0.0164(17)	0.0182(16)	0.027(2)	0.0072(15)	0.0124(15)	0.0038(14)
C12	0.0138(16)	0.0155(15)	0.0164(18)	0.0041(13)	0.0060(14)	0.0020(13)
C13	0.0123(16)	0.0206(17)	0.024(2)	0.0063(15)	0.0058(14)	-0.0007(13)
C14	0.0144(17)	0.0201(17)	0.022(2)	0.0028(14)	0.0004(14)	-0.0058(14)
C15	0.0185(17)	0.0137(15)	0.0181(18)	0.0010(13)	0.0030(14)	-0.0002(13)
C16	0.0116(15)	0.0130(14)	0.0148(17)	0.0015(12)	0.0036(13)	-0.0018(12)
C17	0.0116(15)	0.0098(14)	0.0122(16)	0.0020(12)	0.0025(12)	0.0004(11)
C18	0.0125(15)	0.0107(14)	0.0127(16)	0.0033(12)	0.0019(13)	0.0005(12)
C19	0.0120(15)	0.0137(15)	0.0113(16)	-0.0052(12)	0.0029(12)	-0.0003(12)
C20	0.037(2)	0.0138(16)	0.0178(19)	0.0018(14)	0.0014(17)	0.0030(15)
C21	0.041(2)	0.0179(17)	0.0094(17)	-0.0006(14)	-0.0018(16)	0.0002(16)
C22	0.0160(17)	0.0166(16)	0.0150(18)	-0.0056(13)	0.0044(14)	-0.0019(13)
C23	0.0203(18)	0.0127(15)	0.0155(18)	-0.0026(13)	0.0047(14)	0.0002(13)
C24	0.0161(17)	0.0152(15)	0.0122(17)	-0.0004(13)	0.0018(13)	0.0015(13)
C25	0.0107(15)	0.0157(15)	0.0131(17)	-0.0010(12)	0.0048(12)	-0.0007(12)
C26	0.0175(18)	0.0195(17)	0.033(2)	0.0057(16)	0.0040(16)	-0.0049(14)
C27	0.0148(17)	0.0249(19)	0.023(2)	0.0113(15)	0.0031(15)	0.0034(14)
C28	0.035(2)	0.037(2)	0.032(3)	0.017(2)	0.014(2)	0.011(2)
C29	0.049(3)	0.058(3)	0.037(3)	0.003(2)	0.023(2)	0.012(3)
C30	0.047(3)	0.039(3)	0.036(3)	0.010(2)	0.009(2)	0.010(2)
Cl1	0.0246(5)	0.0211(4)	0.0176(4)	0.0079(3)	0.0032(4)	0.0034(3)
Cl2	0.0108(4)	0.0193(4)	0.0196(4)	-0.0016(3)	0.0030(3)	-0.0018(3)
Cl3	0.0238(5)	0.0195(4)	0.0235(5)	-0.0049(3)	0.0072(4)	0.0075(3)
N1	0.0103(13)	0.0099(12)	0.0129(14)	-0.0008(10)	-0.0005(11)	0.0006(10)
N2	0.0132(13)	0.0089(12)	0.0118(14)	-0.0012(10)	0.0002(11)	-0.0002(10)

N3	0.0125(14)	0.0132(13)	0.0138(14)	0.0005(11)	0.0034(11)	0.0000(11)
N4	0.033(2)	0.037(2)	0.024(2)	0.0077(16)	0.0050(16)	0.0118(17)
O1	0.0135(12)	0.0155(11)	0.0161(13)	0.0038(9)	0.0025(10)	0.0031(9)
O2	0.039(2)	0.050(2)	0.038(2)	0.0065(16)	0.0064(16)	0.0008(16)

Theoretical Studies

General Computational Details:

The initial energy and geometry optimization was carried out at the B3LYP[3] level with the 6-31+G* basis set for non-metal atoms[4] together with the LANL2DZ[5] for In, Br, and Cl atoms. Frequency calculations were carried out at this level to confirm that a minimum had been achieved. To account for solvent effects, a reaction field calculation with radii and non-electrostatic terms with the SMD solvation model was used.[6] All the TD-DFT calculations were carried out using the Gaussian 09 program package.[7]

DFT calculations were used to evaluate both the geometries and energies of different monomers and dimers of the indium complexes. Calculations were carried out with different basis sets (B3LYP/6-31+G* and B3LYP/6-31++G**) and the spectra have been calculated either in vacuum or with the polarizable continuum model to account for solvent effects. To validate our choice of basis sets, geometry optimizations were performed at the B3LYP/6-31+G* level of theory, with the pseudo potential LANL2DZ for the indium, chlorine, and bromine atoms. The agreement between the experimentally determined and the computed structures supports the method used.

- **Geometry Optimization**

The theory level employed was B3LYP/6-31+G*, with the pseudo potential LANL2DZ for the indium, chlorine, and bromine atoms. The geometry optimization performed for the hypothetical dimeric species – [(*p*-MeOAr-BIAN)$_2$InCl$_2$][InCl$_4$] (**A**) and (*p*-BrAr-BIAN)InCl$_2$][InCl$_4$] (**B**) – showed almost identical geometries (both octahedral) and In-N bond distances for both methoxy- and bromo-substituted BIAN indium complexes (Figure S17, top). The calculated In-N bond distances obtained for **A**, ranging from 2.319 - 2.328 Å, are in good agreement with the experimental values observed for dimeric compound **3** (Table S11). In the case of the hypothetical monomeric *p*-MeOAr-BIAN and *p*-BrAr-BIAN species (**C** and **D**, respectively) both showed very similar monomeric optimized geometries (Figure S17, middle). In both cases, a slight asymmetry between the In-N bonds is observed, which is consistent with that also observed in complex **4** (see table S11). Mulliken population analyses show that the net positive charge on the indium atom for the bromo-derivative (**C**) is higher than that of the methoxy containing analogue (**D**) (+0.77 and +0.74 for **C** and **D**, respectively). The greater partial positive charge on the metal center in **C** suggests that formation of the

dimer is more favorable in this case due to electronic reasons. Furthermore, computational studies on the effect of a bound DMF molecule in complexes **C** and **D** in the gas phase indicate greater stabilization in the case of the bromo- than the methoxy-derivative (1.8 kcal/mol *vs*. 0.2 kcal/mol, **C** and **D**, respectively). When the relative energies of the pentacoordinate monomeric complexes **C** and **D** are compared with their DMF solvated hexacoordinate counterparts - both in the gas phase - the **2**-ligated indium complex is more stabilized than its **1**-ligated analogue (1.8 and 0.2 kcal/mol). The consistency observed between the calculated and the experimental values observed indicate that the basis sets used throughout our studies are adequate and represent the complexes under investigation.

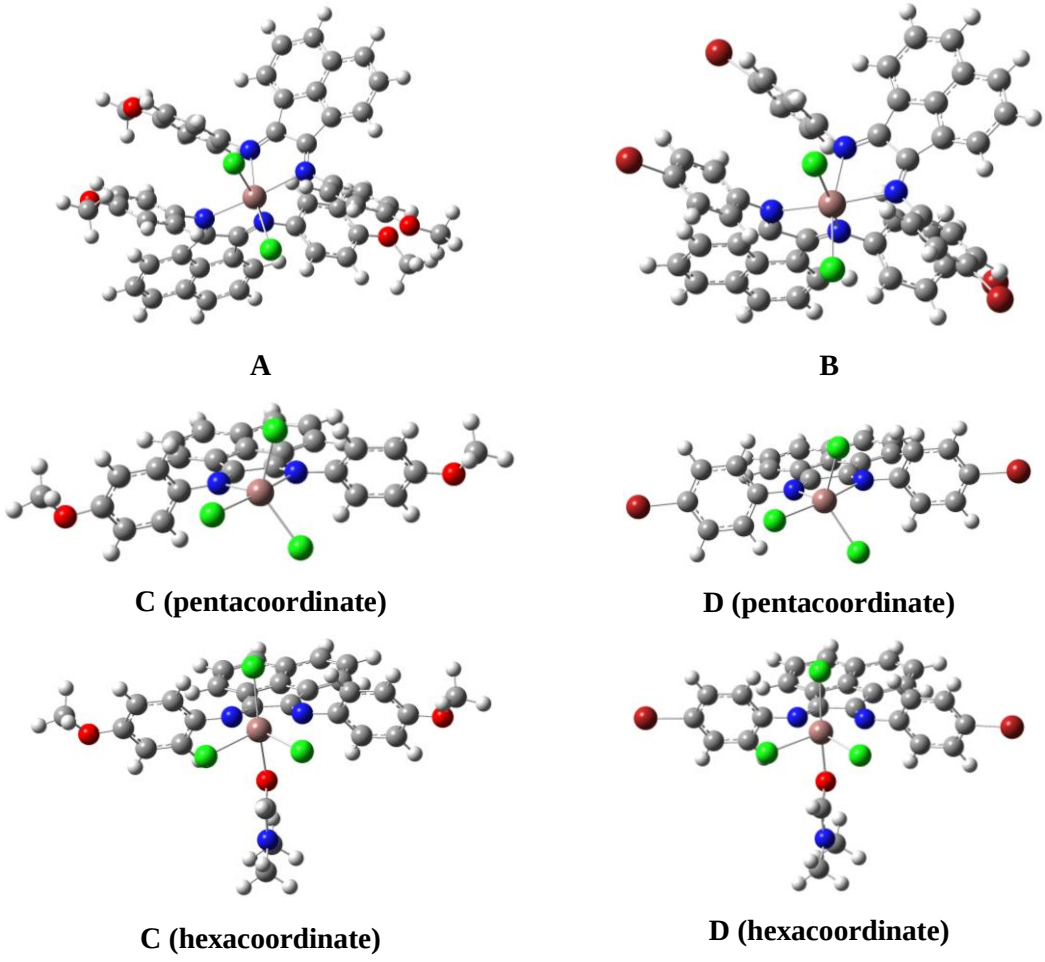

Figure S17. Geometry optimization at the B3LYP/6-31+G*/LANL2DZ level of theory for the indium(III) dimeric (**A** and **B**) and monomeric (**C** and **D**) complexes with ligands **1** and **2**, respectively. Structure **A** corresponds to complex **3,** whereas **B** is the corresponding hypothetical dimeric analogue with ligand **2**. Structure **D (hexacoordinate)** corresponds to complex **4**, whereas **C** is the corresponding hypothetical monomeric analogue with ligand **1** (with and without coordinated DMF)

Table S11. Comparison of the experimental and calculated bond lengths and angles. Geometries were calculated at 6-31+G* theory level.

3 (Exp.)/**A** (calc.)				**4** (Exp.)/**D** (calc.)			
In-N		In-Cl		In-N		In-Cl	
Exp.	Calc.	Exp.	Calc.	Exp.	Calc.	Exp.	Calc.
2.2955	2.30499	2.4126	2.4563	2.390	2.4388	2.4185	2.4187
2.3241	2.32888	2.3963	2.4585	2.301	2.2908	2.4336	2.4255
2.3109	2.31125					2.4286	2.4230
2.3232	2.31974						

- **UV-Vis Spectra Simulations**

TD-DFT calculations were used to predict the electronic absorption spectra of the isolated complexes. The calculations were carried out with different basis sets (B3LYP/6-31+G* and B3LYP/6-31++G**) and the spectra have been calculated either in vacuum or with the polarizable continuum model to account for solvent effects.

Comparisons of the experimental and theoretical spectra for complex A indicate that the TD-DFT calculations correctly describe the electronic absorption bands. It can be observed in Figure S18 that the there is a general spectral shift to higher energies when the solvent is considered. Despite the fact that the differences observed between the calculated spectra with ACN and DMF solvents models are almost negligible, it is necessary to include solvation effect in our theoretical studies. The use of a larger basis set (B3LYP/6-31++G**) and relativistic effects - Douglas–Kroll–Hess theory – did not affect the calculated values (Figure S18). The calculated dominant contributions to the visible absorption maximum for complex **3** (λ_{max} = 461 nm) corresponds to electronic transitions from the HOMO -> LUMO, HOMO-2 -> LUMO, HOMO-1 -> LUMO, and HOMO-1 -> LUMO+1 (Table S13).

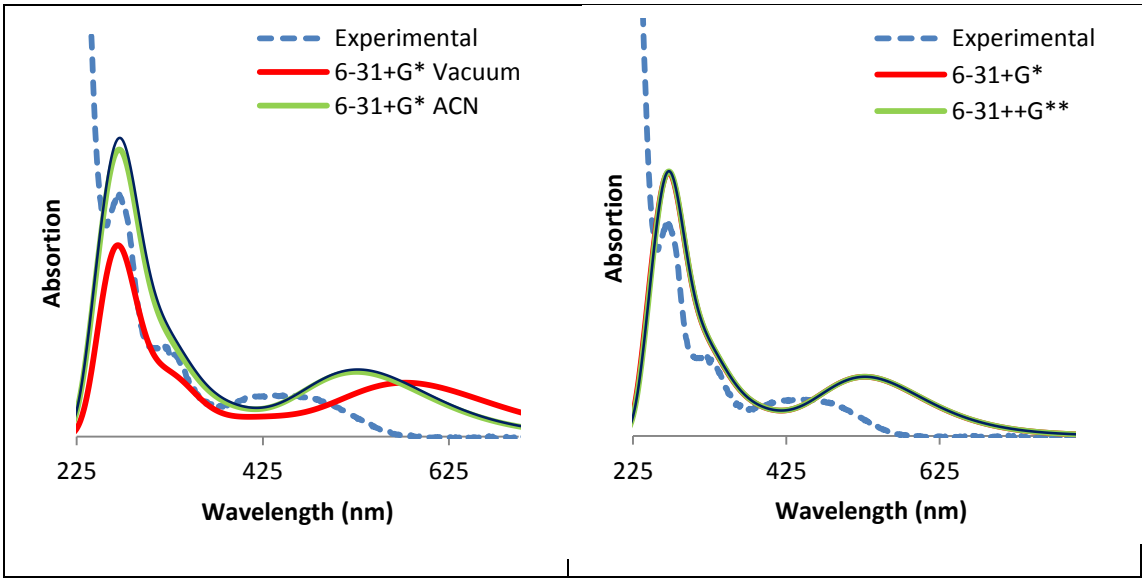

Figure S18. Experimental and calculated absorption spectra in different media (**3** and **A**, respectively) (left). Comparison between the experimental absorption spectrum of **3** and the calculated spectra with different basis sets (right).

Table S12: Orbital contributions to the electronic absorption transitions of **3** using a B3LYP/6-31+G* level of theory; only transitions with oscillator strengths >0.03 have been taken into account.

Transition	λ_{max} (nm)	*f*	Orbital contributions (%)
HOMO-3 →LUMO+1	525	0.1332	2.30
HOMO-2 →LUMO			66.70
HOMO-1 →LUMO			2.69
HOMO-1 →LUMO+1			19.95
HOMO-LUMO			5.17
HOMO-2 →LUMO	570	0.0468	10.87
HOMO-1 →LUMO			4.98
HOMO-1 →LUMO+1			3.29
HOMO-LUMO			72.02
HOMO-LUMO+1			5.94

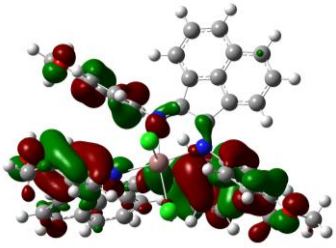

HOMO-2

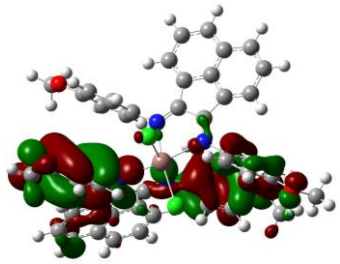

HOMO-1

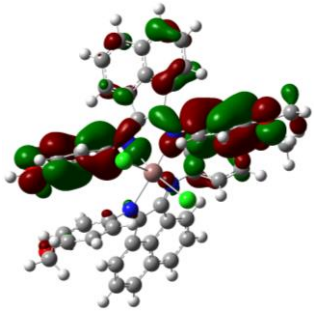

HOMO

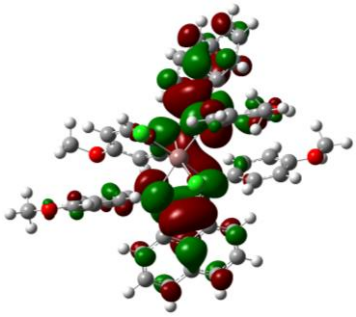

LUMO

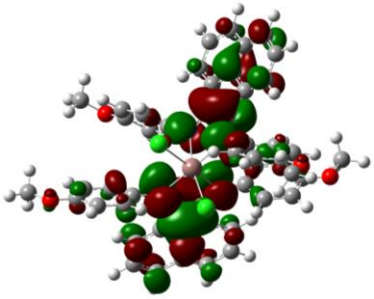

LUMO+1

Figure S19. Highest occupied and lowest unoccupied MOs involved in the transitions that contribute to the calculated absorption spectrum of **3.**

The same trends are observed in the calculated UV-Vis spectra for complex **4**. There is better agreement between the calculated and the experimental data when solvation is included in the computational studies. The use of a larger basis set (B3LYP/6-31++G**) and relativistic effects - Douglas–Kroll–Hess theory – did not affect the calculated values (Figure S20). Our theoretical studies indicate that the visible absorption maximum for complex **4** (λ_{max} = 400 nm) corresponds mainly to the HOMO -> LUMO transition.

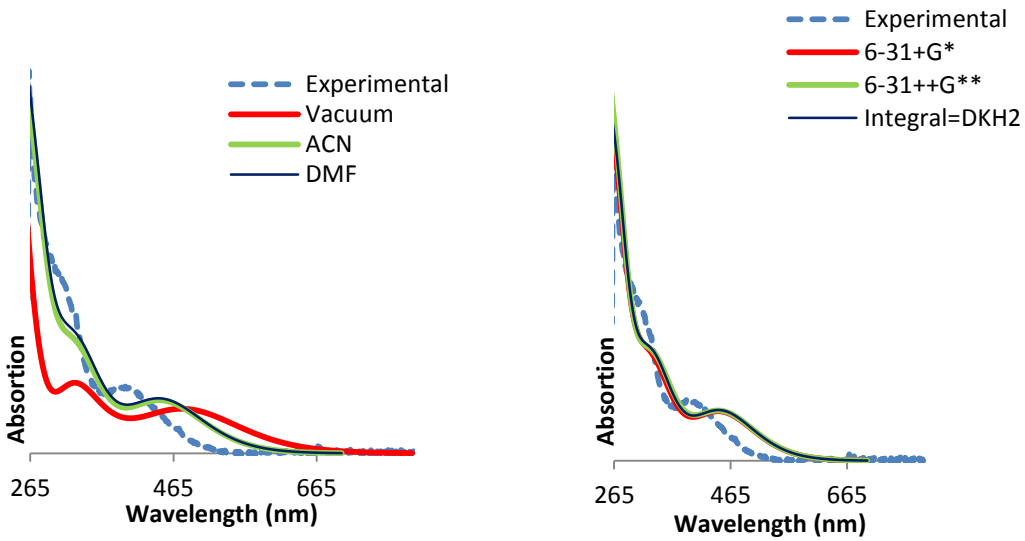

Figure S20. Experimental and calculated absorption spectra in different media (**4** and **A**, respectively) (left). Comparison between the experimental absorption spectrum of **4** and the calculated spectra with different basis sets (right).

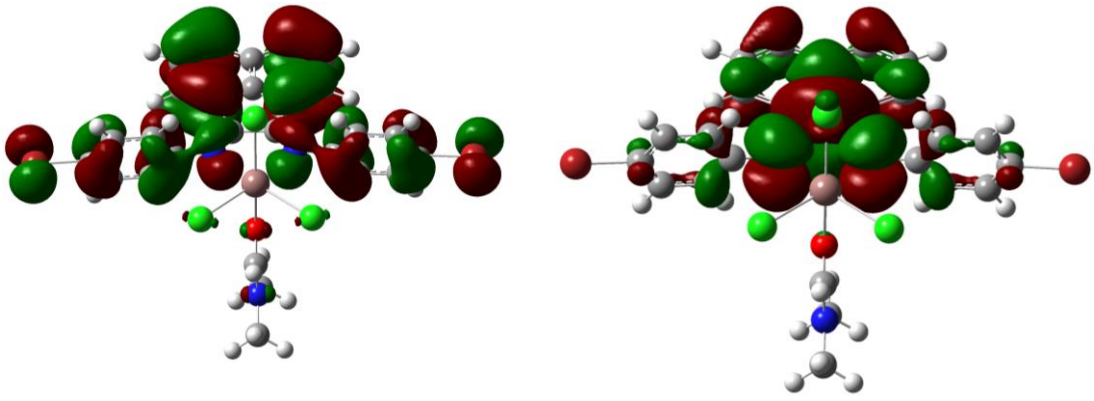

HOMO **LUMO**

Figure S21. Highest occupied and lowest unoccupied MOs involved in transitions that contribute to the calculated absorption spectrum of **4**.

Table S13: Orbital contributions to the electronic absorption transitions of **4** using a B3LYP/6-31+G* level of theory; only transitions with oscillator strengths > 0.03 have been taken into account.

Transition	λ_{max} (nm)	*f*	Orbital contributions (%)
HOMO → LUMO	466	0.0856	98
HOMO-1 → LUMO	427	0.0298	97
HOMO-2 → LUMO	413	0.0273	96

Table S14. B3LYP/optimized Cartesian coordinates of the structures

A

C	6.306433	1.651258	-5.366834
C	5.300712	1.056227	-3.270729
C	4.191047	0.449763	-3.880364
C	3.171819	-0.084681	-3.093458
C	3.272863	-0.069233	-1.697008
C	4.380823	0.545674	-1.087077
C	5.381480	1.107708	-1.865205
C	2.375638	-1.510950	-0.016241
C	3.517788	-2.333668	0.416090
C	4.850952	-2.439436	0.049213
C	5.655370	-3.431806	0.667660
C	5.157289	-4.296064	1.629877
C	3.790774	-4.225144	2.019451
C	3.129070	-5.055080	2.966638
C	1.775621	-4.893060	3.224035
C	0.993750	-3.913919	2.559866
C	1.614142	-3.084293	1.638025
C	3.004462	-3.238631	1.387812
C	1.161697	-2.001915	0.756097
C	-1.175393	-2.016375	1.137630
C	-1.668529	-1.466551	2.329871
C	-2.816981	-1.988426	2.917403
C	-3.495947	-3.062917	2.316035

C	-5.315797	-4.622614	2.448068
C	-3.012390	-3.598294	1.113052
C	-1.858930	-3.069048	0.524871
C	5.156642	2.928365	4.331954
C	3.599520	2.871183	2.505990
C	3.251502	3.365702	1.236124
C	2.095683	2.930844	0.598758
C	1.253494	2.005297	1.235929
C	1.599942	1.501507	2.490772
C	2.769007	1.929861	3.131991
C	-1.082002	2.083939	0.836870
C	-1.512370	3.160743	1.736775
C	-0.869851	3.985753	2.647498
C	-1.629883	4.978477	3.316884
C	-2.984853	5.155595	3.078948
C	-3.668859	4.333050	2.141235
C	-5.038551	4.422159	1.767391
C	-5.559290	3.567832	0.807991
C	-4.774092	2.570121	0.174429
C	-3.438278	2.447625	0.525831
C	-2.902853	3.337027	1.499531
C	-2.311067	1.618836	0.069693
C	-3.265347	0.207563	-1.598408
C	-3.235790	0.308166	-3.000594
C	-4.289376	-0.190279	-3.750857
C	-5.367545	-0.840770	-3.123224
C	-7.453464	-1.996134	-3.397059
C	-5.377285	-0.979347	-1.725665
C	-4.327675	-0.449909	-0.971141
N	2.205119	-0.607616	-0.924427
N	0.006560	-1.484255	0.518462
N	0.062442	1.557764	0.571172
N	-2.166980	0.718253	-0.844048
O	6.331460	1.626947	-3.938553
O	-4.603789	-3.502615	2.971037
O	4.752864	3.359399	3.034512
O	-6.336955	-1.304546	-3.950512
H	7.219658	2.166589	-5.665741
H	5.433755	2.203608	-5.734949
H	4.097279	0.406688	-4.958924
H	2.305011	-0.534737	-3.566608
H	4.436796	0.611550	-0.004632
H	6.231405	1.606572	-1.409696
H	5.292763	-1.785978	-0.692749
H	6.698154	-3.508076	0.373808
H	5.808797	-5.038178	2.084193
H	3.690303	-5.827537	3.486448
H	1.291349	-5.541410	3.948345
H	-0.064553	-3.835095	2.778372
H	-1.142033	-0.645373	2.808088
H	-3.202237	-1.582037	3.847708
H	-5.722668	-4.405329	1.452443
H	-6.135181	-4.800959	3.145313
H	-4.674771	-5.511644	2.399669
H	-3.520944	-4.418434	0.619268
H	-1.494359	-3.468270	-0.416812

H	4.405491	3.190538	5.087755
H	6.085429	3.459747	4.542344
H	5.341431	1.846641	4.351283
H	3.906217	4.090254	0.761593
H	1.835288	3.302492	-0.387773
H	0.954053	0.780190	2.983972
H	3.013100	1.526468	4.108172
H	0.189820	3.893458	2.853173
H	-1.127296	5.624048	4.031094
H	-3.529577	5.935444	3.605179
H	6.306839	0.634436	-5.777772
H	-6.604417	3.659053	0.527087
H	-5.229807	1.926239	-0.567568
H	-2.398077	0.793877	-3.490559
H	-4.291242	-0.104198	-4.832684
H	-5.675114	5.171311	2.231231
H	-8.082081	-2.265643	-4.246432
H	-8.019375	-1.351734	-2.712450
H	-6.182556	-1.498574	-1.218681
H	-4.327065	-0.572966	0.108344
H	-7.134517	-2.906693	-2.874352
Cl	0.431837	1.974161	-2.697333
Cl	-0.454825	-1.791241	-2.756982
In	0.011355	0.060636	-1.211993

C

C	-2.764197	-0.081517	-0.139866
C	-3.411008	0.310267	-1.321760
C	-4.791720	0.205709	-1.426992
C	-5.546542	-0.291400	-0.350214
C	-4.898054	-0.693632	0.825736
C	-3.507106	-0.607676	0.917272
C	-0.712344	1.111183	-0.032763
C	-1.166650	2.509194	0.020357
C	-2.403216	3.132861	0.092346
C	-2.446259	4.546086	0.204970
C	-1.296375	5.320147	0.247585
C	-0.012773	4.710655	0.188340
C	1.247867	5.366578	0.260282
C	2.420995	4.630187	0.228772
C	2.425633	3.214708	0.112849
C	1.214580	2.548661	0.026975
C	0.803608	1.131418	-0.016556
C	0.011870	3.304698	0.067360
C	2.841952	-0.094734	-0.058306
C	3.553596	-0.802743	0.916233
C	4.938794	-0.947922	0.811249
C	5.616736	-0.421656	-0.297230
C	4.894538	0.254187	-1.297630
C	3.523325	0.419217	-1.176865
N	-1.335959	-0.019852	-0.045731
N	1.429253	0.010046	0.038217
H	-2.827748	0.673374	-2.163505
H	-5.305535	0.485845	-2.341373
H	-5.452883	-1.102119	1.662160

H	-3.004288	-0.953901	1.814447
H	-3.328025	2.570110	0.063178
H	-3.416302	5.031899	0.259533
H	-1.373156	6.401250	0.335382
H	1.286206	6.449462	0.349387
H	3.374610	5.146468	0.293750
H	3.369515	2.683517	0.092909
H	3.022990	-1.227844	1.761599
H	5.467897	-1.485588	1.589541
H	5.427147	0.619949	-2.170162
H	2.964863	0.904819	-1.971500
In	-0.051628	-1.905095	0.040266
Cl	-1.938818	-3.426234	-0.108796
Cl	0.637832	-2.215047	2.359340
Cl	1.161992	-2.469950	-1.979881
O	6.958421	-0.521193	-0.503342
O	-6.892249	-0.351709	-0.550011
C	7.743885	-1.251574	0.433955
H	7.415470	-2.296502	0.496156
H	8.766224	-1.211966	0.055068
H	7.704194	-0.791231	1.429516
C	-7.709920	-0.923999	0.466107
H	-8.728341	-0.893943	0.075903
H	-7.423207	-1.963974	0.665392
H	-7.656686	-0.340649	1.394487

C with DMF

C	2.797248	0.264755	-0.227667
C	3.526947	0.453368	0.956645
C	4.907560	0.299615	0.959953
C	5.581355	-0.040780	-0.225332
C	4.852791	-0.237372	-1.406462
C	3.462763	-0.107520	-1.398955
C	0.747095	1.435502	0.050988
C	1.173858	2.826730	0.301596
C	2.394254	3.480559	0.352377
C	2.408408	4.886733	0.548486
C	1.244726	5.626702	0.684734
C	-0.024699	4.988051	0.620361
C	-1.299133	5.615207	0.697568
C	-2.457454	4.864832	0.573012
C	-2.432642	3.458910	0.376190
C	-1.206935	2.816216	0.312998
C	-0.770313	1.429106	0.057260
C	-0.019330	3.588173	0.435340
C	-2.813312	0.243214	-0.207384
C	-3.485210	-0.124458	-1.376337
C	-4.874322	-0.264217	-1.373954
C	-5.594758	-0.082139	-0.185524
C	-4.913978	0.253380	0.997127
C	-3.534488	0.416958	0.984293
C	-0.003735	-2.723161	2.065050
C	0.202289	-1.785434	4.311109
C	0.061965	-4.248697	3.959162
N	1.376346	0.350650	-0.230321
N	-1.392957	0.339628	-0.220597

N	0.079678	-2.906579	3.387158
O	0.008153	-1.599252	1.513806
H	3.004755	0.693530	1.878823
H	5.483187	0.422540	1.872501
H	5.345408	-0.518772	-2.329902
H	2.891894	-0.291647	-2.303482
H	3.330620	2.946672	0.246212
H	3.368574	5.393549	0.589229
H	1.297757	6.703040	0.830177
H	-1.360387	6.691017	0.843695
H	-3.421668	5.362995	0.623689
H	-3.365147	2.916558	0.279296
H	-2.919962	-0.297695	-2.286551
H	-5.372241	-0.541967	-2.295646
H	-5.483152	0.364625	1.915195
H	-3.006459	0.652931	1.904236
H	-0.089790	-3.638825	1.473870
H	0.206987	-0.856780	3.740753
H	1.134836	-1.870790	4.881812
H	-0.641465	-1.782757	5.011626
H	-0.787890	-4.358496	4.643234
H	0.989625	-4.436604	4.512623
H	-0.028698	-4.988238	3.160606
In	-0.004350	-1.496584	-0.758170
Cl	1.889097	-3.087591	-0.693961
Cl	-0.011324	-0.653159	-3.098111
Cl	-1.889426	-3.098726	-0.692168
O	-6.947536	-0.217779	-0.071369
O	6.935827	-0.166200	-0.120765
C	-7.689139	-0.632357	-1.213660
H	-7.351465	-1.613334	-1.570775
H	-8.726714	-0.700978	-0.882600
H	-7.612779	0.101963	-2.026127
C	7.671384	-0.584722	-1.265576
H	8.711880	-0.644050	-0.941983
H	7.337432	-1.570581	-1.612575
H	7.583962	0.142864	-2.082956

B

C	5.409938	-0.096108	-3.077593
C	4.258176	-0.569085	-3.706544
C	3.135975	-0.879632	-2.937322
C	3.191606	-0.745068	-1.545263
C	4.346741	-0.255515	-0.923896
C	5.463010	0.074328	-1.693362
C	2.014145	-2.010417	0.093581
C	2.971746	-3.050011	0.492019
C	4.260060	-3.397069	0.112488
C	4.860925	-4.538044	0.703261
C	4.205993	-5.314279	1.647570
C	2.879898	-4.992717	2.050612
C	2.074181	-5.701976	2.984527
C	0.779668	-5.285995	3.261566
C	0.201338	-4.154231	2.633663
C	0.965671	-3.438290	1.723936
C	2.296474	-3.857969	1.449958

C	0.729838	-2.268633	0.874689
C	-1.553500	-1.775644	1.290851
C	-1.870381	-1.163841	2.509067
C	-3.118176	-1.385290	3.098427
C	-4.038250	-2.213818	2.455413
C	-3.733054	-2.823738	1.238445
C	-2.486868	-2.598196	0.648520
C	4.038118	2.214134	2.455065
C	3.732899	2.824104	1.238130
C	2.486708	2.598559	0.648207
C	1.553375	1.775926	1.290486
C	1.870283	1.164087	2.508679
C	3.118062	1.385566	3.098057
C	-0.729749	2.269317	0.873735
C	-0.965321	3.439497	1.722318
C	-0.200887	4.155618	2.631817
C	-0.778848	5.288032	3.258885
C	-2.073076	5.704482	2.981208
C	-2.878898	4.995019	2.047540
C	-4.204705	5.316998	1.643883
C	-4.859757	4.540450	0.699911
C	-4.259332	3.398735	0.110121
C	-2.971305	3.051273	0.490260
C	-2.295887	3.859570	1.447804
C	-2.014026	2.011060	0.092630
C	-3.191808	0.744668	-1.545193
C	-3.136214	0.876954	-2.937479
C	-4.258599	0.565693	-3.706138
C	-5.410543	0.094228	-3.076385
C	-5.463619	-0.073964	-1.691868
C	-4.347175	0.256630	-0.923004
N	2.027167	-1.055096	-0.772553
N	-0.293119	-1.518132	0.658595
N	0.293008	1.518355	0.658226
N	-2.027245	1.055260	-0.772989
H	4.225014	-0.684697	-4.784447
H	2.227438	-1.234664	-3.413877
H	4.371691	-0.119358	0.153321
H	6.358737	0.460054	-1.218016
H	4.815425	-2.821619	-0.617824
H	5.869283	-4.805948	0.402406
H	4.704079	-6.178853	2.078684
H	2.476684	-6.581793	3.480009
H	0.182678	-5.846823	3.974426
H	-0.818721	-3.874894	2.869810
H	-1.144677	-0.525352	3.004540
H	-3.364721	-0.918149	4.046164
H	-4.457149	-3.462976	0.744240
H	-2.242274	-3.041788	-0.311762
H	4.456974	3.463387	0.743949
H	2.242109	3.042169	-0.312067
H	1.144596	0.525564	3.004130
H	3.364622	0.918415	4.045784
H	0.818986	3.875942	2.868368
H	-0.181789	5.849015	3.971565
H	-2.475267	6.584829	3.476001

H	-5.867881	4.808684	0.398565
H	-4.814803	2.823044	-0.619925
H	-2.227574	1.230802	-3.414706
H	-4.225432	0.679554	-4.784226
H	-4.702471	6.182136	2.074234
H	-6.359476	-0.458562	-1.215853
H	-4.372106	0.122103	0.154420
Cl	0.798251	1.768700	-2.589998
Cl	-0.798171	-1.769255	-2.589592
In	-0.000019	-0.000038	-1.093000
Br	-5.786803	-2.506299	3.263168
Br	-6.973152	-0.353915	-4.148368
Br	6.972343	0.350948	-4.150383
Br	5.786692	2.506579	3.262825

D

C	-2.773972	-0.092262	-0.017217
C	-3.461135	-0.220011	-1.226203
C	-4.856437	-0.270436	-1.225905
C	-5.538697	-0.209911	-0.011982
C	-4.859402	-0.115736	1.201305
C	-3.463980	-0.059386	1.197154
C	-0.715963	1.078666	0.003599
C	-1.161456	2.476959	-0.008395
C	-2.395971	3.107819	-0.041622
C	-2.430975	4.525508	-0.044511
C	-1.276286	5.294207	-0.009952
C	0.004931	4.677090	0.025233
C	1.270081	5.327443	0.071379
C	2.439859	4.584782	0.107780
C	2.437534	3.164538	0.091051
C	1.221441	2.505122	0.040756
C	0.804629	1.091465	0.038166
C	0.022200	3.266691	0.016912
C	2.845652	-0.108037	0.063977
C	3.539554	-0.500048	1.214218
C	4.933861	-0.587551	1.183681
C	5.609372	-0.313420	-0.003457
C	4.924507	0.037036	-1.166399
C	3.533531	0.141413	-1.130447
N	-1.337568	-0.049371	-0.017451
N	1.419870	-0.029894	0.092061
H	-2.911896	-0.292744	-2.159973
H	-5.397498	-0.369270	-2.160807
H	-5.402571	-0.095028	2.140069
H	-2.916999	-0.004720	2.133899
H	-3.323099	2.547753	-0.062085
H	-3.397501	5.020152	-0.071354
H	-1.348889	6.379068	-0.008241
H	1.315642	6.413594	0.080197
H	3.395129	5.100212	0.146753
H	3.377265	2.625470	0.113881
H	2.991494	-0.740844	2.118408
H	5.477798	-0.878924	2.075877
H	5.460192	0.216393	-2.092527
H	2.981247	0.380027	-2.033500

In	-0.070562	-1.957903	-0.001257
Br	-7.491958	-0.273843	-0.009823
Br	7.560366	-0.441474	-0.047660
Cl	-2.011398	-3.391808	-0.167463
Cl	0.747593	-2.395828	2.239763
Cl	1.044368	-2.305575	-2.124309

D with DMF

C	2.811132	0.247059	-0.182406
C	3.530018	0.274759	1.017586
C	4.921727	0.161550	1.000182
C	5.572190	0.024998	-0.224640
C	4.865321	-0.025523	-1.424523
C	3.472933	0.070462	-1.402441
C	0.765868	1.407152	0.113409
C	1.198539	2.789472	0.388898
C	2.423742	3.430686	0.470269
C	2.445111	4.831471	0.700236
C	1.284253	5.576081	0.839513
C	0.010520	4.949126	0.748067
C	-1.261320	5.580778	0.833260
C	-2.424180	4.840395	0.688272
C	-2.406821	3.439474	0.458790
C	-1.183624	2.793680	0.383473
C	-0.754599	1.409564	0.110836
C	0.008493	3.554596	0.529081
C	-2.802147	0.254243	-0.190227
C	-3.459948	0.069714	-1.411311
C	-4.852433	-0.023691	-1.437830
C	-5.563714	0.037273	-0.241071
C	-4.917545	0.182179	0.985074
C	-3.525739	0.292891	1.006695
C	0.024466	-2.945295	1.889439
C	-0.173548	-2.195186	4.205352
C	-0.010370	-4.620306	3.653242
N	1.386444	0.320320	-0.168116
N	-1.377434	0.324174	-0.171417
N	-0.047876	-3.235899	3.191465
O	0.000480	-1.779470	1.430168
H	3.002800	0.369517	1.962698
H	5.484222	0.175955	1.927867
H	5.384346	-0.155377	-2.368053
H	2.898740	0.004208	-2.321420
H	3.357484	2.892591	0.360607
H	3.407704	5.330945	0.763336
H	1.343827	6.648333	1.009727
H	-1.317802	6.653251	1.003125
H	-3.385241	5.343401	0.746502
H	-3.342006	2.904817	0.344706
H	-2.882605	-0.004281	-2.327712
H	-5.368162	-0.159620	-2.382304
H	-5.483492	0.205016	1.910492
H	-3.002085	0.394455	1.953066
H	0.112755	-3.808705	1.224519
H	-0.203302	-1.223443	3.713010
H	0.681309	-2.234315	4.891040

H	-1.094772	-2.344309	4.780936	Br	-7.515942	-0.101354	-0.277077
H	-0.931740	-4.862979	4.195300	Cl	1.915862	-3.053290	-0.890644
H	0.845658	-4.773244	4.320840	Cl	0.003621	-0.427581	-3.066638
H	0.083774	-5.291905	2.797269	Cl	-1.907301	-3.052495	-0.880595
In	0.003798	-1.498610	-0.818424				
Br	7.524332	-0.116795	-0.254553				

REFERENCES

[1] C. S. K. Mak, H. L. Wong, Q. Y. Leung, W. Y. Tam, W. K. Chan, A. B. Djurišić, *J. Organomet. Chem.* **2009**, *694*, 2770-2776.

[2] A. L. Gottumukkala, J. F. Teichert, D. Heijnen, N. Eisink, S. van Dijk, C. Ferrer, A. van den Hoogenband, A. J. Minnaard, *J. Org. Chem.* **2011**, *76*, 3498-3501.

[3] a) A. D. Becke, *Phys. Rev. A*, **1988**, *38*, 3098 –3100; b) C. Lee, W. Yang, R. G. Parr, *Phys. Rev. B*, **1988**, *37*, 785 – 789; c) A. D. Becke, *J. Chem. Phys.* **1993**, *98*, 5648 – 5652.

[4] W. J. Hehre, L. Radom, J. A. Pople, P. v. R. Schleyer, Ab Initio Molecular Orbital Theory, Wiley, New York, 1986.

[5] P. J. Hay and W. R. Wadt, *J. Chem. Phys*., **1985**, *82*, 270-83

[6] A. V. Marenich, C. J. Cramer, and D. G. Truhlar, J. *Phys. Chem. B*, **2009**, *113*, 6378-96.

[7] a) Gaussian 09, Revision D.01, M. J. Frisch *et al.* Gaussian, Inc., Wallingford CT, 2009; b) Lee, C. T.; Yang, W. T.; Parr, R. G. *Phys. Rev. B* **1988**, *37*, 785; c) Becke, A. D. *J. Chem. Phys.* **1993**, *98*, 5648; d) Becke, A. D. *Phys. Rev. A* **1988**, *38*, 3098.